

UNIVERSIDAD SAN FRANCISCO DE QUITO USFQ

Colegio de Posgrados

Design and Realization of a Measuring Node for Gravimetric Applications

**Tesis en torno a una hipótesis o problema de investigación y su
contrastación**

Juan José Jiménez Villalba

**Francesco Lamonaca, Ph.D.
Director de Trabajo de Titulación**

**Anna Albano, Ph.D.
Co-Director de Trabajo de Titulación**

Trabajo de titulación de posgrado presentado como requisito
para la obtención del título de Máster en Nanoelectrónica

Quito, 6 de enero de 2023

UNIVERSIDAD SAN FRANCISCO DE QUITO USFQ
COLEGIO DE POSGRADOS

HOJA DE APROBACIÓN DE TRABAJO DE TITULACIÓN

Design and Realization of a Measuring Node for Gravimetric Applications

Juan José Jiménez Villalba

Nombre del Director del Programa: Luis Miguel Prócel
Título académico: Doctor of Philosophy
Director del programa de: Maestría en Nanoelectrónica

Nombre del Decano del colegio Académico: Eduardo Alba
Título académico: Doctor of Philosophy
Decano del Colegio: Colegio de Ciencias e Ingenierías

Nombre del Decano del Colegio de Posgrados: Hugo Burgos
Título académico: Doctor of Philosophy

Quito, enero de 2023

© DERECHOS DE AUTOR

Por medio del presente documento certifico que he leído todas las Políticas y Manuales de la Universidad San Francisco de Quito USFQ, incluyendo la Política de Propiedad Intelectual USFQ, y estoy de acuerdo con su contenido, por lo que los derechos de propiedad intelectual del presente trabajo quedan sujetos a lo dispuesto en esas Políticas.

Asimismo, autorizo a la USFQ para que realice la digitalización y publicación de este trabajo en el repositorio virtual, de conformidad a lo dispuesto en la Ley Orgánica de Educación Superior del Ecuador.

Nombre del estudiante: Juan José Jiménez Villalba

Código de estudiante: 00215761

C.I.: 1721783007

Lugar y fecha: Quito, 6 de enero de 2023.

ACLARACIÓN PARA PUBLICACIÓN

Nota: El presente trabajo, en su totalidad o cualquiera de sus partes, no debe ser considerado como una publicación, incluso a pesar de estar disponible sin restricciones a través de un repositorio institucional. Esta declaración se alinea con las prácticas y recomendaciones presentadas por el Committee on Publication Ethics COPE descritas por Barbour et al. (2017) Discussion document on best practice for issues around theses publishing, disponible en <http://bit.ly/COPETheses>.

UNPUBLISHED DOCUMENT

Note: The following graduation project is available through Universidad San Francisco de Quito USFQ institutional repository. Nonetheless, this project – in whole or in part – should not be considered a publication. This statement follows the recommendations presented by the Committee on Publication Ethics COPE described by Barbour et al. (2017) Discussion document on best practice for issues around theses publishing available on <http://bit.ly/COPETheses>.

ACKNOWLEDGEMENTS

A special acknowledgment is extended to Anna Albano, who with her knowledge and experience on the equipment allowed the development of the gravitational station. Another acknowledgment is extended to Francesco Lamonaca and Domenico Luca Carnì, as with their guidance and advice the project took shape. Lastly to my family, since without their unconditional support none of this could have ever happened.

RESUMEN

El sur de Italia, en particular Calabria, es una zona de interés geofísico debido a su elevada actividad sísmica y volcánica. La comparación constante de los registros de las amplitudes y fases de las señales de marea con los modelos de los registros gravitacionales son útiles para detectar a tiempo acciones volcánicas y sísmicas. Esta investigación propone la creación de un nodo de medida para aplicaciones gravimétricas diseñado para garantizar una adquisición multiparamétrica de las señales de marea y de la magnitud que influye en su adquisición.

El nodo es capaz de monitorar: la aceleración gravitacional, la inclinación en los ejes N-S y E-O, la temperatura y la presión barométrica ya que estos parámetros que tienen efectos sobre las aceleraciones gravitacionales según diversos modelos. Para la aceleración gravitatoria se utilizó el gravímetro G-1089 de LaCoste & Romberg. Tiene un rango operativo de 7000 mGal, con una resolución de 0,005 mGal y una precisión de 0,04 mGal. Para la inclinación, se utilizó el inclinómetro Modelo 714 de Applied Geomechanics. Es capaz de realizar mediciones con un rango angular de $\pm 8000,0$ μrad , una resolución de 0,1 μrad y una linealidad del 2% dentro del intervalo de medida.

Como sistema de adquisición, para este nodo de medida se utilizó la unidad de adquisición y conmutación de datos Agilent 34970A. Que tiene una resolución de 6,5 dígitos (22 bits) y una precisión del 0,004% para medir la tensión continua. El retardo de lectura se midió en 7,99 ms con $\sigma = 2,06$ ms para canales consecutivos y se despreció ya que el periodo de muestreo del sistema fue de 5s en esta aplicación. Se utilizó Labview para, convertir la hora y los datos en Coordenadas de Tiempo Universal (UTC), comunicarse con la unidad de adquisición de

conmutación mediante directivas SCPI, escalar las magnitudes y almacenar las diferentes medidas.

En particular, se confrontaron mediciones a las variaciones gravitacionales debidas a los desplazamientos de las mareas en el globo terráqueo, ya que los valores teóricos pueden darnos un punto de partida correcto para determinar si los datos adquiridos por el nodo son precisos y utilizables para futuras investigaciones. Los resultados preliminares obtenidos, tras algunos filtrados de ruido y aproximaciones polinómicas, demostraron seguir las variaciones teóricas de las mareas en el mes de abril de 2022, lo que nos permite concluir que el nodo gravitatorio está funcionando correctamente, y que los datos obtenidos por el mismo pueden ser utilizados en próximas investigaciones en el área de la geofísica.

Palabras clave: Gravimetría, gravímetro, inclinómetro, sistema de adquisición de datos, retardo de lectura, nodo de medición, adquisición de datos, procesamiento de datos.

ABSTRACT

Southern Italy, in particular Calabria, is an area of geophysical interest due to its high seismic and volcanic activity. Constant comparison of records of the amplitudes and phases of the tidal signals with models of the gravitational records are useful to timely detect volcanic and seismic actions. This research proposes the creation of a measurement node for gravimetric applications designed to guaranty a multiparametric acquisition of the tidal signals and of the magnitude influencing their acquisition.

The node is able to monitor gravitational acceleration, inclination on the N-S and E-W axis, temperature and barometric pressure monitoring since these parameters that have effects on the gravitational accelerations according to diverse models. For the gravitational acceleration, the gravimeter G-1089 from LaCoste & Romberg was utilized. It has an operating range of 7000 mGal, with a resolution of 0.005 mGal and an accuracy of 0.04 mGal. For the inclination, the tiltmeter Model 714 from Applied Geomechanics was utilized. It is capable of measurements with an angular range of ± 8000.0 μ rad, a resolution of 0.1 μ rad and a linearity of 2% within the full span.

As an acquisition system, the Agilent 34970A data acquisition and switching unit was utilized for this measurement node. Which has a 6.5 digits of resolutions (22 bits) and a 0.004% accuracy for measuring DC voltage. Reading delay was measured to 7.99 ms with $\sigma = 2.06$ ms for consecutive channels and was neglected as the sampling period of the system was 5s. Labview was used for, converting time and data into Universal Time Coordinates (UTC), communicate with the switching acquisition unit via SCPI directives, scaling the magnitudes and storing the different measurements.

In particular, we plan to apply our measurements into gravitational variations due to tidal shifts in the globe, as the theoretical values can give us a correct starting point to determine if the data acquired by the node is accurate and usable for further research in the future. The preliminary obtained results, after some noise filtering and polynomial approximations proved to follow the theoretical tidal variations in the month of April 2022, which allows us to conclude that the gravitational node is working properly, and that the data obtained by it can be utilized in upcoming research in the area of geophysics.

Key Words: Gravimetry, gravimeter, tide meter, data acquisition system, reading delay, measurement node, data acquisition, data processing.

TABLE OF CONTENTS

Acknowledgements	5
Resumen	6
Abstract	8
Table of Contents	10
Tables index	12
Figure Index	13
Introduction	16
Chapter 1: Introduction of Gravimetry Applications and Equipment.....	17
1. Gravimeter.....	17
A. Operational Principle.....	18
B. Applications.....	24
2. Tiltmeter	26
A. Operational Principle.....	27
B. Applications.....	28
Chapter 2: Implementation of the Gravitational Monitoring System	29
1. Equipment	29
A. Gravimeter LaCoste & Romberg Model G-1089	30
B. Tiltmeter: Platform and Surface Mount Model 712	39
C. Agilent 34970A Data Acquisition / Switching Unit.....	44
D. Other equipment	52
2. Software Implementation	55
A. File Creation Block:.....	57
B. Time Based Control Structures.....	61
C. Read From Device:	63
D. Write into .txt SubVI	66
Chapter 3: Results	68
1. Folder Structure and graphs:	68
2. Gravimetrical Monitoring	73
3. Additional Measured Parameters:	77
4. Confrontation with tidal monitoring from a different station:	80
Chapter 4: Conclusions	81

Bibliography.....	82
-------------------	----

TABLES INDEX

Table 1: Monitoring of Gravimeters Temperature.....	37
Table 2: Color Coding of Tiltmeter.....	41
Table 3: Channel Delay Results	51

FIGURE INDEX

Figure 1. Time Diagram of a Free-Falling Object	19
Figure 2. Equilibrium of a Spring mass System	20
Figure 3. Sensitivity relationship to the elongation of the spring.	21
Figure 4. Torque equilibrium of a zero-length spring system.....	23
Figure 5. Seismic activity in from 1984 to 2014 in southern Italy	26
Figure 6. Single axis tiltmeter layout.	27
Figure 7. Double axis tiltmeter layout.....	27
Figure 8. Acquisition System Diagram.....	30
Figure 9. The LaCoste & Romberg Model G-1089	30
Figure 10. Polypropylene Thermal Isolation Enclosure	33
Figure 11 Gravimeter Top View Diagram	34
Figure 12. Gravimeter Top View Photo.....	34
Figure 13. Eyepiece Photo	38
Figure 14. Temperature LCD monitoring	38
Figure 15. Tiltmeter Layout from User Manual	40
Figure 16. Tiltmeter Photograph.....	40
Figure 17. Agilent 34970A Data Acquisition / Switching Unit.....	44
Figure 18. Agilent 34970A Data Acquisition / Switching Unit Backside	46
Figure 19. Channel Expansion Card Side View.....	47
Figure 20. Channel Expansion Card Top View	47
Figure 21. Datta acquired from the first 4 Channels.....	48
Figure 22. Data Acquired from 8 Channels	49
Figure 23. Sensors of Gravitational Station	54
Figure 24. Computer, Power Supply and Acquisition Unit.	55
Figure 25. LabVIEW Front End Interface	56
Figure 26. LabVIEW Backend View	57
Figure 27. Create Files SubVI Icon.....	57

Figure 28. Create Files SubVI pt1.....	58
Figure 29. Create Files SubVI pt2.....	58
Figure 30. Create Files SubVI pt3.....	60
Figure 31.Header Example of .txt.....	61
Figure 32. UTC Time Transformation	61
Figure 33. Condition for 5 sec Aquisition.....	61
Figure 34.Condition for New File Creation	62
Figure 35. Reading and Writing Data	63
Figure 36. Communication with Switching unit pt1.	65
Figure 37. Communication with Switching unit pt2.....	65
Figure 38. Write into .txt SubVI.	66
Figure 39. File Organization	68
Figure 40 Folder File's Example.....	69
Figure 41. -12V Channel monitoring example	69
Figure 42. +12V Channel monitoring example.....	70
Figure 43. Tiltmeter EW Channel monitoring example.....	70
Figure 44.Tiltmeter NS Channel monitoring example.....	71
Figure 45. Temperature Channel monitoring example	71
Figure 46. Central Level Channel Monitoring Example.....	72
Figure 47. Lateral Level Channel Monitoring Example	72
Figure 48. Feedback Channel Monitoring Example	73
Figure 49. Gravitational Acceleration Raw data of January and February 2022.....	73
Figure 50. Inclination of North-South Axis	74
Figure 51. Inclination of East West Axis	75
Figure 52.Temperature Monitoring for January 2022.....	76
Figure 53. Pressure Monitoring for January 2022	76
Figure 54. Lateral Level Signal Monitoring	77
Figure 55. Central Level Signal Monitoring	78
Figure 56.. +12 V Supply Monitoring.....	78
Figure 57. -12 V Supply Monitoring.....	79

Figure 58. Gravimetric Variation based on theoretical tidal fluctuation. 80

INTRODUCTION

Around 20 years ago, in the Università della Calabria, geological studies were done utilizing LaCoste y Romberg Gravimeter Model-1089, a good choice at the time LaCoste & Romberg gravimeters were highly desired due to its accuracy, and build quality, although a steep price. After a period of inactivity of more than ten years, twenty years later a first attempt to create a measurement node for gravimetry is done with this thesis with this equipment. The final aim is to create a worldwide network of gravimetric measurement nodes for a global study of gravity changes in the world.

After initially connecting the device in September 2021, the measurement devices were checked to determine if they were still operational, hardware was chosen to measure the signals and software was developed to monitor gravitational parameters from this measuring equipment. Initial successful results were obtained. The metrological characteristics were evaluated by comparing the tidal variation measured by the gravimeter and the theoretical one imposed by the moon. Unfortunately, the vibrations introduced by the building structures hid these signals and a new location for the node were established in the ground of Cube 41C of University of Calabria.

With a combination of other metrological monitoring station located on the same University (Cube 41B) that has several metrological sensor equipment, the creation of a metrological station with gravimetry sensors was finally achieved by the end of December 2022.

The thesis is organized as following. Chapter 1 presents general concepts of gravimetry, the measurement instruments, their architectures, and applications. Chapter 2 describes the hardware and software architecture of the gravimetric measurement node, the achievable accuracy. Chapter 3 shows the results of the gravimetric signals acquired in the period January and February 2022. Conclusion follow in Chapter 4.

CHAPTER 1: INTRODUCTION OF GRAVIMETRY APPLICATIONS AND EQUIPMENT

Gravimetry is the discipline in charge of studying the acceleration of gravity in, or near, Earth's surface and its variations (Timmen, 2010). This discipline has several advantages for mankind is fundamental for mapping (Olesen, 2022), navigation, and universal timing (G. D'Agostino, 2005) (Snadden, 1998), which is utilized for urban and rural development, transportation (L. Kallivroussis, 2002), construction (Carlos Duque, 2008) [7], and other human activities. Also, the monitoring of Earth's changes in the oceans (A. Albano, 2015), ice caps and atmosphere (A.ThomasJ.Gebhart, 1994) can be fundamental, prevention, and mitigation and alarm rising of natural disasters such as the ones generated by seismic (T.M.Niebauer, 2011) or volcanic activity (Vajda, 2016).

1. Gravimeter

A gravimeter is an accelerometer with the purpose of measuring the strength of the gravitational field, in our case, the acceleration due to earth's gravity. The units of measurement according to the International System (SI) is the meter per second-squared [m/s^2]. However, another common unit of measurement is the *Gal* which conversion rate is 1 cm/s^2 . Since earth's gravity is not constant through all the surface, previous research on the zone of Arcavacata where this station is located in (Biolcati E., 2013), the accepted value for this zone is $g = 9.80106699 \pm 9 \times 10^{-8} \text{ ms}^2$ obtained with absolute gravimetry. Absolute gravimeters are the ones that report a local value for the gravity in the position where they are placed. Relative gravimeters utilize a measurement obtained by networks of gravimeters on different locations determine a local measurement. This increases accuracy of the measurement but increases the complexity (Biolcati E., 2013).

A. Operational Principle

There are several methods utilized by gravimeters to measure the acceleration of an object regarding the gravitational force at which an object is subjected to. In (World Documents. LaCoste & Romberg Gravimeters, 2015) the most common methods utilized by gravimeters are evaluated. The three most common methods are the following:

a) *Free-Falling Object*

The simplest method utilized is to measure the fall of an object (Biolcati E., 2013). By measuring the fall time on an object and the distance it falls, the following equation can be utilized to determine the acceleration of this given object (LaCoste M. G., 2006).

$$x = x_0 + v_0t + \frac{1}{2}gt^2$$

This equation corresponds to the uniform accelerated movement of a free-falling object. By measuring this object on three different instances in the same fall, the variables of the initial position x_0 , and initial velocity v_0 are not required for the calculation of the acceleration. With the following equations, the gravitational acceleration g can be easily determined.

$$\begin{cases} x_1 = x_0 + v_0t_1 + \frac{1}{2}gt_1^2 \\ x_2 = x_0 + v_0t_2 + \frac{1}{2}gt_2^2 \\ x_3 = x_0 + v_0t_3 + \frac{1}{2}gt_3^2 \end{cases} \quad (2)$$

$$\Rightarrow g = 2 \frac{(x_3 - x_1)(t_2 - t_1) - (x_2 - x_1)(t_3 - t_1)}{(t_3 - t_2)(t_2 - t_1)(t_3 - t_1)} \quad (3)$$

Figure 1. demonstrates the variables required for the calculation of the acceleration.

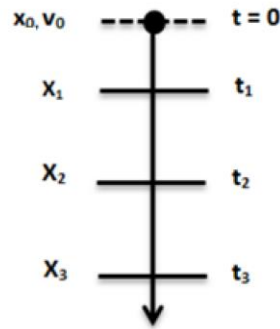


Figure 1. Time Diagram of a Free-Falling Object (World Documents. LaCoste & Romberg Gravimeters, 2015)

This method is utilized in to determine absolute gravity in gravimeters such as the model Migro-g LaCoste A-10 which is a transportable instrument, or the Migro-g Lacoste FG-5 (LaCoste M. G., 2006) which has a higher sensitivity and accuracy, but it is not a transportable system. In this case the measurement accuracy depends on the accuracy with which the distance and the time can be measured.

b) Static Spring–Mass System

The second method is the spring mass system. This system suspends a given mass by a spring and it is elongated due to the gravitational force until it achieves equilibrium. This is shown on Figure 2.

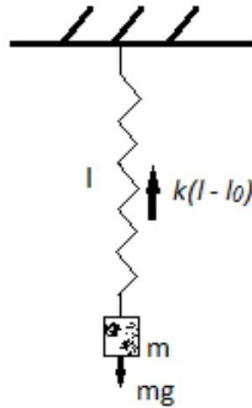


Figure 2. Equilibrium of a Spring mass System (World Documents. LaCoste & Romberg Gravimeters, 2015).

The acceleration will be determined by Hooke's law. In equilibrium, the net force of the system adds up to zero as shown on equation 4:

$$mg - k(l - l_0) = 0 \quad (4)$$

Where:

- m corresponds to the mass of the object
- k corresponds to the elongation constant of the spring
- l is the distance the spring is elongated in the equilibrium position
- l_0 is the initial elongation of the spring without the application of any force
- g is the gravitational force.

This method is utilized on relative gravimeters (B Richter, 2013), which means that the measurement obtained for the gravitational force is compared with other measurements of other gravimeters. The variation of the gravitational acceleration Δg will proportionally vary accordingly to the variation of the elongation of the spring Δl as shown on equation 5.

$$\Delta g = \frac{g}{l - l_0} = \frac{m}{k} \Delta l$$

As these equation shows, the sensitivity is directly proportional to the elongation. Therefore, a spring with a low stiffness, and a low elongation constant will stretch out a further distance increasing the resolution of the gravimeter. This is shown on Figure 3.

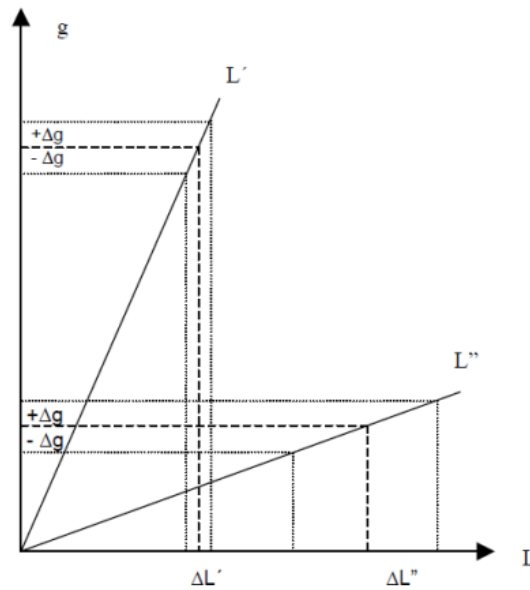


Figure 3. Sensitivity relationship to the elongation of the spring (World Documents. LaCoste & Romberg Gravimeters, 2015).

Formula description of this relationship is shown on equation 6.

$$\Delta g = \frac{g}{l - l_0} = \frac{m}{k} \Delta l \quad (6)$$

Therefore, the resolution and uncertainty of these types of devices depend on the accuracy with which the distance variation can be measured (B Richter, 2013).

c) Zero-Length Springs

More modern gravimeters utilize zero-length springs (LaCoste L.). Zero-length springs are specially designed coils that would have a virtual length of zero if they were not subjected to any force and are also able to sensitive to compression forces. This makes them efficient at monitoring oscillating quantities such gravitational variations. with high accuracy any force. Research has been done on the materials of zero-lengths springs, either quartz or metal. Considering those studies, LaCoste & Romberg decided to go for metallic stings on their measurement devices (D. Zhong, 2013) as springs have longer life spawn. Gravimeters based on this principle where initially developed by LaCoste back in the first iterations of the company in the year 1934 (LaCoste L. J., 1935).

The diagram of how the layout of these systems is shown on Figure 4. A lever is fixed in point one end, and a mass is suspended on the other. The spring creates a reaction forge to the weight to counteract the tension that is produced by the mass suspended on the lever. However, the mass does create a variation on angles α and δ . By measuring these angles, the gravitational force and finally acceleration can be calculated (LaCoste L. J., 1935).

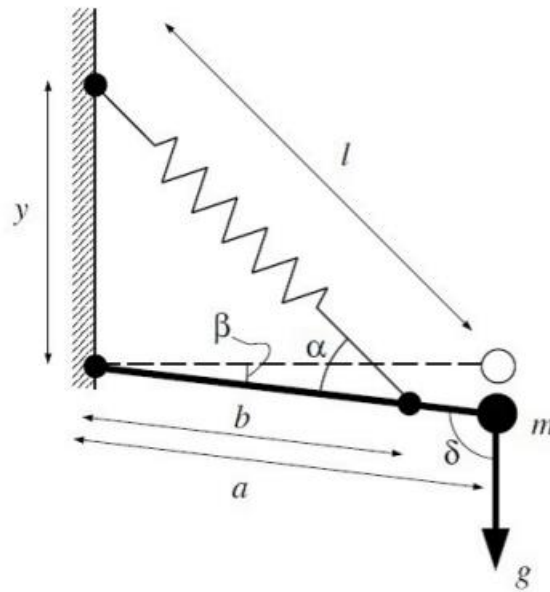


Figure 4. Torque equilibrium of a zero-length spring system. (World Documents. LaCoste & Romberg Gravimeters, 2015).

In equilibrium, the sum of all the torques of the system equals to zero. Equation 7 shows the direct and inverse relationship of the variables.

$$\begin{aligned}
 mga \cos(\beta) &= k (l - l_0) b \sin(\alpha) & (7) \\
 &= k (l - l_0) b \frac{y}{l} \cos(\beta)
 \end{aligned}$$

Equation 8 shows the calculation of the gravitational acceleration.

$$g = \frac{kb}{ma} \left(1 - \frac{l_0}{l}\right) y \quad (8)$$

Gravimeters developed by LaCoste & Romberg, as the one utilized on the system implemented on this research metallic springs, which are useful due to its long duration on the field. These gravimeters are also valued for their portability, making them common for on fields applications (J. C. Harrison, 1984).

As on the previous example, the resolution and uncertainty of the gravitational force is dependent on the ability to measure the elongation of the spring (LaCoste L. J., 1935).

B. Applications

Gravitational anomalies can be caused by a diversity of reasons such as changes in earth tides (A. Albano, 2015), atmospheric density (Simpson, 1982), barometric pressure, and seismic events (A. Albano, 2015). It must be noted that for these applications extreme resolution is required. For the more extreme applications like on determining geological constants in (Biolcati E., 2013), results with 8 decimal points and a resolution of 90nms^{-2} are used to determine local g values in southern Italy.

Gravimetry is utilized in diverse fields of study. In the mining field, gravimetry can be used to determine the material below earth's surface. The measurement of the gravitational field can allow scientist to determinate the distribution and composition of masses within the interior of the Earth's crust, allowing the detection of hydrocarbons and other minerals (Peters, 1987).

Another application of gravimetry is the monitoring of the variation of the Earth's tides (R. Sulzbach, 2021). The water displacement of the water in the oceans leads to several fields of study. For example, tide monitoring can allow prediction on the sea levels on coastal cities, where hydroelectric plants exploit this phenomenon to produce energy (A. Cazenavea, 2009) . Also, tide monitoring allows for the monitoring of variations mineral displacement in the oceans,

and its effect on the flora and fauna of area. This gives valuable information for sustainable phishing and preservation of diverse marine creatures. Tidal currents also influence the temperature, precipitation, wind, and pressure of studied areas (Jing Tong, 2018). The study of it which can shine a light on the metrological status of the studied area and its possible repercussions in the weather which is used for navigation of sea craft as well as possible natural disasters related to atmospheric variations such as tropical storms (Jing Tong, 2018). Tidal variation is affected by the position of the sun and the moon relative to the Earth, as their gravity affects the tides and allows scientist to pinpoint the location of this celestial bodies (A. Albano, 2015).

Lastly, the G as gravitational changes travel at the speed of light, they are used in warning systems in seismic zones. Gravimeters are constantly used to study seismic and volcanic activity as an important area of study where gravimetry has proven extremely helpful is in the monitoring of natural disasters (A. Albano, 2015). Gravimetry used in warning systems in seismic and volcanic zones as it studies events, event frequency tectonic plate movements and earthquake risk estimations (Woollard, 1959). To study volcanic activity gravimetry is used to study the underground mass distribution and movement that occur on these types of events.

In the south of Italy, where this system will be implemented, research of this field is a common risk zone of both seismic and volcanic activity. Figure 5 shows seismic activity in the region of south of Italy. Each circle marks a seismic event, higher than 3.4 on the Richter scale and within 50Km of the earth's surface since 1984 to 2014 (A. Albano, 2015).



Figure 5. Seismic activity in from 1984 to 2014 in southern Italy (A. Albano, 2015)

2. Tiltmeter

A tiltmeter is an extremely sensitive inclinometer used to measure the vertical inclination of the ground or of any structure that it is attached to (Review of Scientific Instruments, 2008). The units utilized to measure could either be an arcminute or an arcsecond. An arcminute is equivalent to 1/60 of a degree while an arc second corresponds to 1/3600 of a degree. Modern electronic tiltmeters use microelectromechanical systems that allow the user to perform inclination monitoring in singular or dual axis modes (Review of Scientific Instruments, 2008) .

A. Operational Principle

The operational principle of a tiltmeter consists of a tube with a small pocket of air inside and filled with an electrolytic substance. Electrodes are placed a configuration such as that the air bubble that its inside is barely touching both electrodes. As the device is tilted, the bubble is moved from the zero position and the electronic resistance changes. Then, by measuring the electronic resistance, the inclination of the device can be determinate. Figure 6 and 7 show examples of single and dual axis tiltmeters respectively. Note that both configurations have a common mode terminal to use as reference.

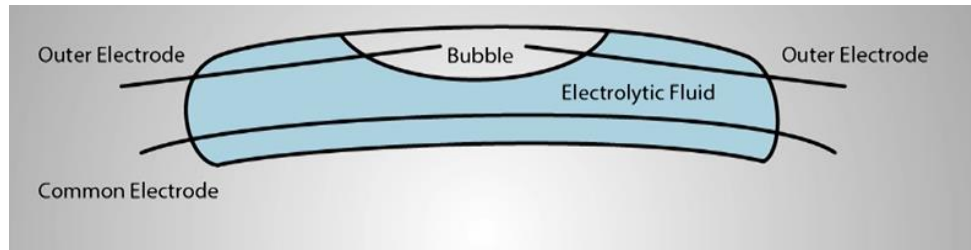


Figure 6. Single axis tiltmeter layout.

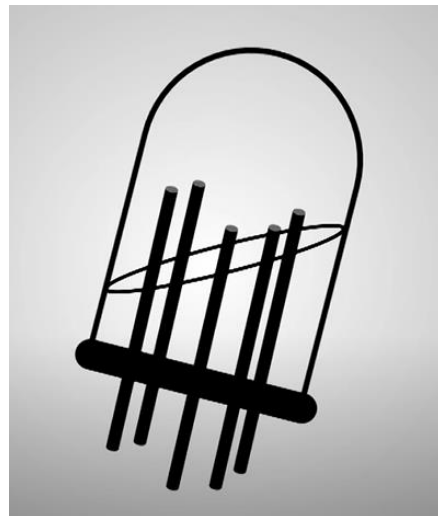


Figure 7. Double axis tiltmeter layout.

In (Jie Liu, 2022) devices utilizing this measurement principle arrived to stability at a resolution of 1.8 nanoradians an uncertainty below 5%.

B. Applications

Tiltmeters are used to gather information on volcanoes all over the world, like Alaska, America, Japan, Italy etc. As volcanoes are preparing for an eruption, magma fluctuations occur inside the volcano. As magma is shifting position, seismic activities can be detected by gravimeters. However, magma relocation inside the volcano also starts to make surface inclination as magma keeps accumulating in underground pillars from the inside the volcano. In the surface, an array of tiltmeters can detect this movement and estimate the amount of magma that is being displaced and estimate the potential risk. This information is extremely valuable as it can rise an alarm before a natural catastrophe happens (Aline Peltiera, 2011).

By applying the same principle, in the extraction of natural gas tiltmeters are to estimate the amount of displaced gas on an area gathered by monitoring the inclination of the surface. This process is called hydraulic fracturing or fracking, and it's a well stimulation technique where bedrock is broken down with pressurized liquid to extract petroleum or natural gas embedded on the gravel (V.Cayol, 1997).

CHAPTER 2: IMPLEMENTATION OF THE GRAVITATIONAL MONITORING SYSTEM

The objective of this project is to create a measuring station that would give researchers, as much information as it can be possible for a monitoring of gravitational variations and its evolution in time. The end user will receive a list of information which will include: the gravitational field, the inclination of the surface in two axis, North-South, and East-West orientation, the temperature and pressure of the environment. In the future, to furthermore complete the atmospheric station, sensors for relative humidity, pressure, wind velocity and the amount of rain the area will also be included.

This way, a combination of on-site measurements as well information from meteorological live stations in the nearby areas will complete a metrological station located in Aravacata, Rende Cosenza in the south of Italy. This has been an area of interest by geologists, as mentioned before due to the high seismic activity location around active volcanic zones as the southern on Italy is. Particularly, this situation is located in Universita della Callabria: Latitude: 39° 21' 29.39" N, Longitude: 16° 13' 21.00" E.

1. Equipment

At the moment, the station includes a gravimeter, in particular the LaCoste & Romberg Model G1089, and a tiltmeter, the 712 Model from the 700-Series made by Applied Geomechanics which has an integrated temperature sensor. Both sensory elements are connected to the Agilent 34970A Data Acquisition and Switch Unit which is controlled by a computer running software that controls the data acquisition, as well as the processing and storage received by these sensors. Figure 8 shows the connection scheme of this monitoring system as well as the flow of information:

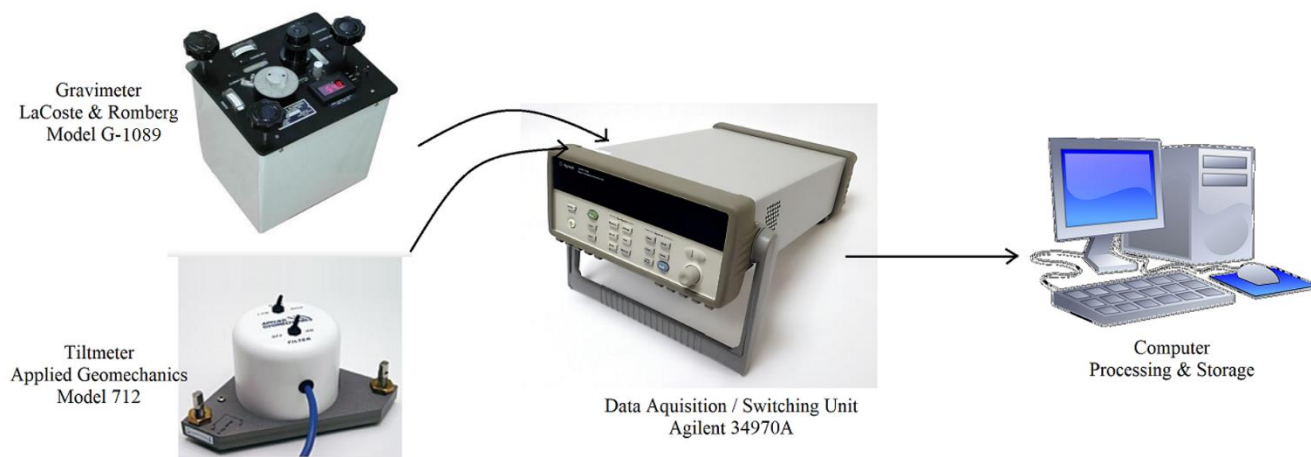


Figure 8. Acquisition System Diagram

The following section will detail each element and its capabilities.

A. Gravimeter LaCoste & Romberg Model G-1089

The LaCoste & Romberg Model G-1089, is showed in Fig. 9



Figure 9. The LaCoste & Romberg Model G-1089

a) *Technical Specifications:*

Obtained from the datasheet in (LacCste And Romberg, 2004), the technical specifications are the following:

- Range: 7000 mGal
- Resolution: 0.005 mGal
- Accuracy: 0.04 mGal or better
- Repeatability: 0.01 to 0.02 mGal
- Drift: 1.0 mGal per month or less
- Length: 7-3/4 inches (19.7 cm)
- With: 7 inches (17.8 cm)
- Height: 9-7/8 inches (25.1 cm)
- Weight: 7 pounds (3.2 kg)
- Weight of the battery: 5 pounds (2.3 kg)
- Weight of meter, battery and carrying case: 22 pounds (10.0 kg)

b) *General Information:*

Several considerations that should be taken into account about this the G-1089 gravimeter. For starters, it has an extremely high range of measurement of 7000 mGal (World Documents. LaCoste & Romberg Gravimeters, 2015). The mGal is utilized for high accuracy measurements on the gravitational acceleration and its equivalence to the international system of units is shown on equation 9, while equation 10 shows the sensitivity

$$1 \text{ Gal} = 0.01 \text{ ms}^{-2} \quad (9)$$

The range of this particular model is higher than other models done by LaCoste & Romberg, such as the model D gravimeters which have a range of 2000 mGal (World Documents. LaCoste & Romberg Gravimeters, 2015).

However, the accuracy of the reading of this gravimeter, can be influenced by a variety of factors. The three main causes of errors according to studies done to LaCoste & Romberg gravimeters are (A. Albano, 2015): temperature fluctuations, shocks, and calibration errors. These factors can make variations such as that the precision is affected up to $\pm 0.05 \mu\text{ms}^{-2}$.

To avoid shocks, the gravimeter was placed on an excluded area with low traffic of people. This way, the gravimeter will not be disturbed by people who can pass and accidentally disturb the extremely sensitive device. When it comes to temperature, the gravimeter is extremely sensitive to temperature fluctuations. The internal temperature of the gravimeter must remain around below the $56.00 \text{ }^\circ\text{C}$ to maintain the accuracy and longevity of the device. The ideal internal temperature is $55.85 \text{ }^\circ\text{C} \pm 0.02 \text{ }^\circ\text{C}$. (A. Albano, 2015). The importance of maintaining the temperature is so detrimental for the correct functioning of the device, that it comes with an external battery that will maintain the gravimeter in the correct operating voltage for the device not to go below the desired temperature range as long stretches of high temperatures might damage the device.

In order to further isolate the gravimeter from temperature fluctuations two actions were taken. The first one was to locate the gravimeter on the basement of the building. Other than isolating the monitoring system of other people who might disturb the acquisition of data, this location will allow the gravimeter to remain cool on the summer, where in Cosenza-Calabria, where this gravimeter is located, temperatures of up to 40°C or higher can be reached. The second action that was taken was to isolate the gravimeter with the ambient temperature by

enclosing it in a polypropylene box as done previously on (A. Albano, 2015). This will furthermore isolate the gravimeter from external temperature fluctuations. Figure 10 shows the isolation box where the gravimeter is placed:

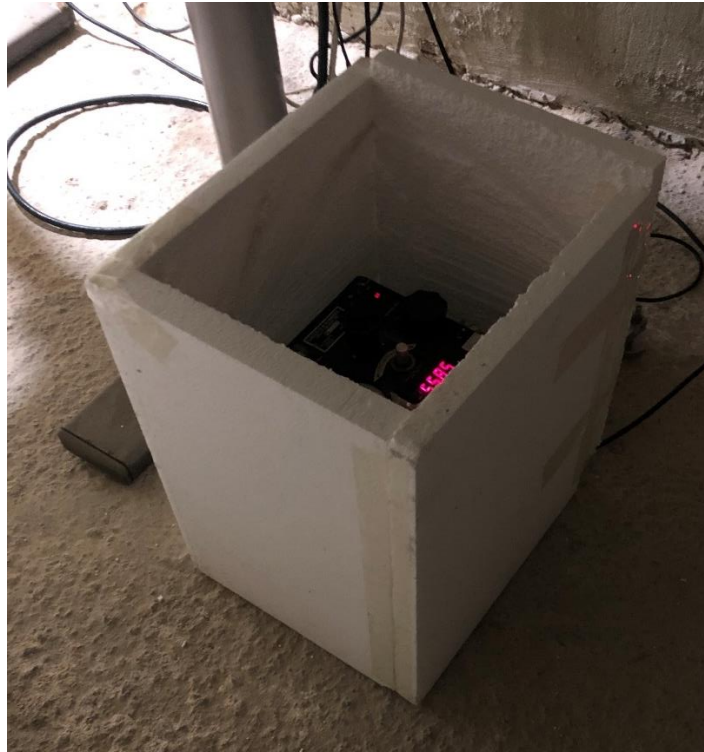


Figure 10. Polypropylene Thermal Isolation Enclosure

c) Calibration of the device:

Lastly, for the calibration of the device, the procedure detailed below was followed. In order to (LaCoste M. G., 2006) explain the steps taken for this calibration a diagram and photo are shown on figures 11 & 12.

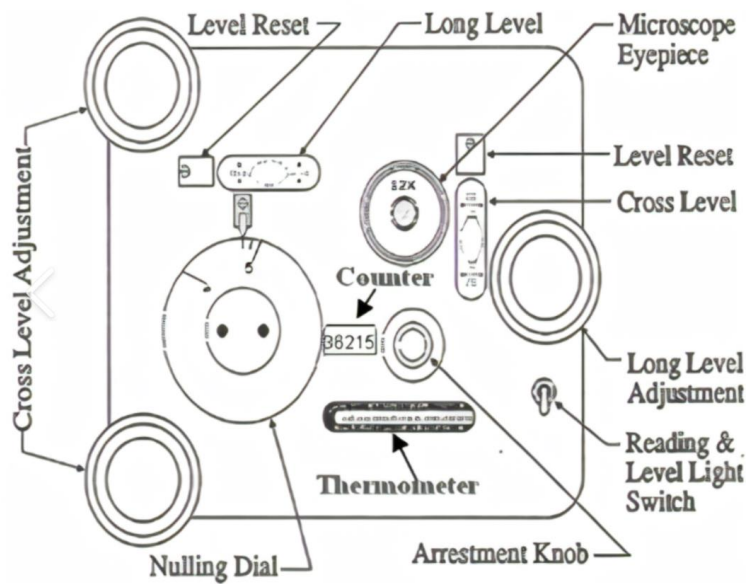


Figure 11 Gravimeter Top View Diagram



Figure 12. Gravimeter Top View Photo

1. For starters, a verification that the central dial is positioned on the clamped position before doing any movement of the gravimeter.
2. The gravimeter was then moved to the location where it is going to be set. The left side of the gravimeter (as shown on the image) should be aligned with the North-South Axis.
3. Set the feedback lever in the MVR OFF position, it is located on the top right of the gravimeter and turn off the reading & level light switch.
4. Connect the cables on the back of the gravimeter. There should be three cables connected to the back, corresponding to the central level, left level and feedback channel. CL, LL and FB correspondingly.
5. Connect the gravimeter and the battery to the electrical power.
6. Move the dial on the bottom left (see image) to the “G” position.
7. Verify on the LCD screen that the gravimeter is has a constant voltage of 12V.
8. Wait at least for 12 hours in order for the battery to fully charged (as indicated by the LED lights on the battery charger) and also for the gravimeter it to achieve a desired temperature of 55.88°C. This was verified by moving the lower left dial into the “B” position and check the desired temperature is achieved on the LCD screen. For this implementation, the waiting time was more than a week before the gravimeter was manipulated further.
9. Once the set-up time has passed, turn on the reading & level light switch. The level bubbles will now be easily visible.
10. With the light turned on, turn slowly the two dials of the cross level until the bubble on the cross-level section is positioned in the middle.

11. Turn the long level dial until the bubble in the long level is set up on the middle.
12. Turn the arrestment knob counterclockwise until the mass is fully unclamped
13. While looking through the 15x microscopic eyepiece, turn the nulling dial until the reading line arrives to the value of 2.5.
14. Turn off the light from the reading & level light switch.
15. Turn on the feedback from the lever in the top left position of the gravimeter and place it on the bottom position. The one corresponding to 10V.
16. Finally, enclose the gravimeter with the polyurethane isolation box.

After this set up process was done, constant controls were done to control that the internal temperature of the gravimeter did not surpass the 56.00 °C. This was done constantly after the gravimeter was set on the final position and several variables were taken into account. The bubble levels were checked and kept centered during the next weeks after the set up. The reading line was controlled, and it remained constant around the and the control of the first couple of weeks can be shown on Table 1.

Date	Hour	Bubble Levels	Reading Line (oculare)	Reading Number (36___)	Gravity measures Dial in <i>D</i>	Temperature [°C] Dial in <i>B</i>
2021-12-21	22:52	OK	2.5	36600	-1417.9	55.84
2021-12-22	13:59	Ok	2.3	36600	-1247.7	55.87
2021-12-22	16:47	Ok	2.25	36000	-1212.9	55.87
2021-12-23	14:42	Ok	2.3	36001	-1227.2	55.86
2021-12-27	15:21	Ok	2.3	36601	-1220.5	55.85
2021-12-28	17:30	Ok	2.3	36601	-1308.9	55.85
2021-12-29	14:50	Ok	2.3	36601	-1160.1	55.85
2021-12-30	21:09	Ok	2.3	36601	-1448.5	55.87
2022-01-02	21:06	Ok	2.3	36601	-1343.2	55.88
2021-01-04	22:30	Ok	2.3	36601	-1310.1	55.87

Table 1: Monitoring of Gravimeters Temperature.

Figure 13 is an image taken the 18 of February of 202. and shows how the gravimeter has kept the reading line, initially settled on the value of 2.3 measured by looking at the eyepiece.

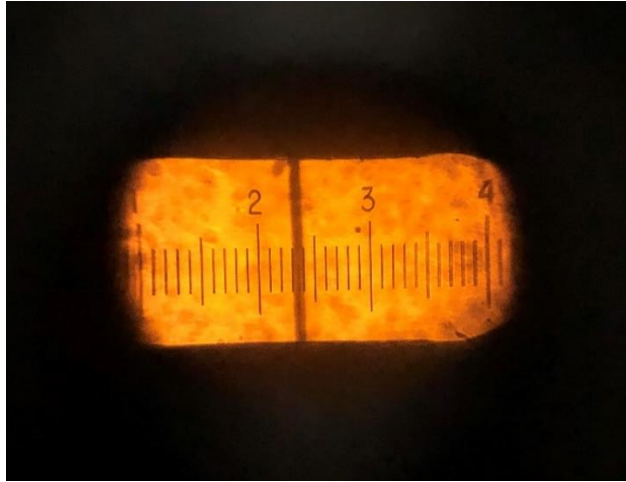


Figure 13. Eyepiece Photo

Figure 14. how the gravimeter after two months of operation has kept on the desired temperature range, with a measurement of 55.85°C.



Figure 14. Temperature LCD monitoring

B. Tiltmeter: Platform and Surface Mount Model 712

a) General information:

The tiltmeter utilized for the creation of this measuring node for gravitational applications in this case of the family of the 700-Series Platform and Surface Mount Tiltmeters from Applied Geomechanics. In particular, the one utilized for this project is the 714 model (Applied Geomechanics). This tiltmeter has a are dual-axis analog output signal. It is designed for high-sensitivity and low power consumption. The advantage of the 700 Series tiltmeters from Applied geomechanics is that it is made for long durability, and reliability under rugged field conditions, which makes it perfect for projects in remote locations where it will provide years of trouble-free service in industrial and laboratory applications. In previous research, this tiltmeter has been used on hydraulic fracture applications (Moradi, Angus, & Sharma, 2022) and seismic activity (A. Albano, 2015) (Pater, Koning, Maxwell, & Walters, 2008.),

The 714 model is constructed with a stainless-steel base plate, and a stainless-steel cover dome that shields the sensors, PC board, connectors, and switches. It has adjustable legs that are used for leveling the tiltmeter on any hard horizontal surface. However, these adjustable legs are also knotted which means that it can also be utilized for setting it on vertical application. The nuts will ensure the adjustment of the surface mount tiltmeter and will guarantee that the tiltmeter will lock in place for long-term measurements.

Figure show the tiltmeter and well as its layout view with the dimensions.

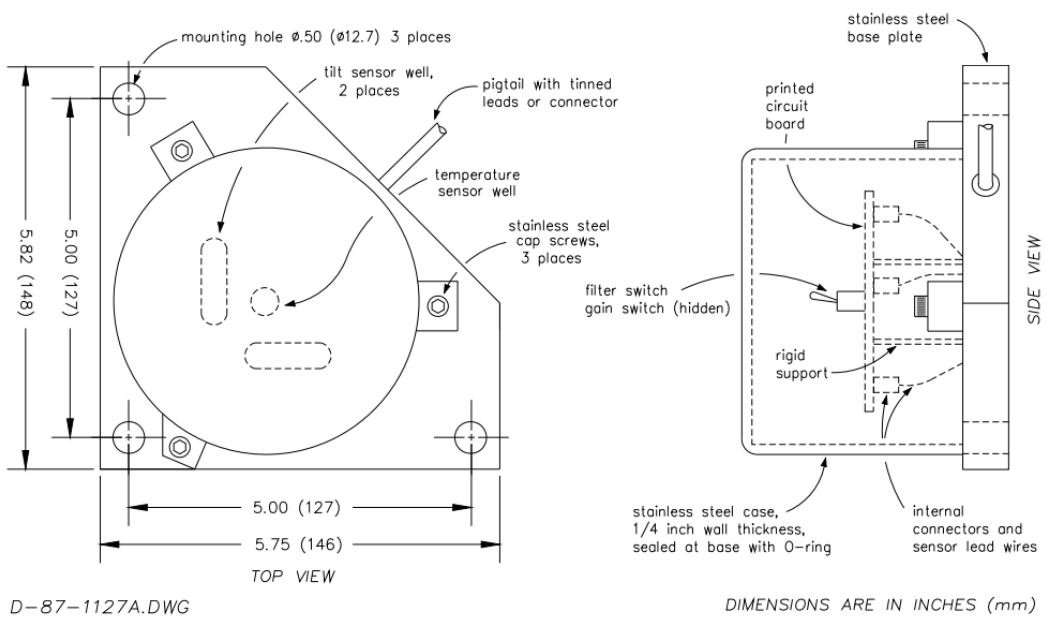


Figure 15. Tiltmeter Layout from User Manual (Applied Geomechanics).



Figure 16. Tiltmeter Photograph

One of the advantages of this Tiltmeter is that it has several external parameters such as temperature, and the voltage supplies that powers the sensor. Table 2 was obtained from the datasheet of the device indicates the color coding of the different signals that come out from the gravimeter on (Applied Geomechanics).

Connector Pin Assignments and Cable Color Coding

Bendix Pin #	Amphenol Pin #	Wire Color	Signal/Function
H	B	red	+12 VDC in
A	I	black	Power ground†
B	F	violet	-12 VDC in
G	G	blue	Channel +Y out
K	E	brown	Channel -Y out
J	C	gray	Channel -X out
C	A	green	Channel +X out
F*	-	-	Case or cable shield (earth ground)
E	D	white	Signal ground†
D	H	yellow	Temperature out

†Signal and Power grounds are common on the tiltmeter electronics circuitry.

* Pin F is connected to the tiltmeter case in Models 701-1, 711-1, 714-1, 716-1 and to the drain wire (shield) of the tiltmeter cable in Models 701-2, 711-2, 714-2, 716-2, 702, 712, 715 and 717.

Table 2. Color Coding of Tiltmeter (Applied Geomechanics).

As we can see from the table above, the tiltmeter has 7 signals useful for the monitoring in the device in the gravitational station. Two dual signals are utilized for the monitoring of the two axes that the gravimeter measures.

At the moment of set up, a compass was utilized in order to align the Y axis of the gravimeter with the North-South axis of the earth and the X axis was aligned with the East-West direction. Additionally, the voltage supply was also connected to the switching unit in order to control the power supply of the tiltmeter. This will allow future researchers the monitoring of the

power supply in case an anomaly occurs on the measurement of the tiltmeter. This will also be useful to determine if a power blackout occurred as it will allow researchers to pinpoint the exact time frame at which it happened. For the power supply monitoring, the tiltmeter has three signals: a +12V power supply, a -12V supply, and a ground connection which is the same for the supply of the tiltmeter, as well as for the output signals of the tiltmeter.

Lastly, this tiltmeter has an external temperature sensor which allows the monitoring of the ambient temperature where it is located. In total, the tiltmeter has 7 signals that can be monitored.

The basic operating principle of this tiltmeter is that it contains two electrolytic level sensors (one for each tilt axis) that produce a change in resistance in response to a rotation of the sensor. By using a voltage divider to sense the resistance change, the electronics in the tiltmeter amplify, actively rectify, and filter the AC sensor output to form a high-level DC signal that is proportional to the tilt angle. Some technical features that this tiltmeter has are the following:

- The sensing of the change in tilt angle with is done with an electrolytic sensor
- All electronics are on a single printed-circuit board.
- The external connections of the circuit board are gold-plated in order to increase the operation life of the tiltmeter and a noise-free operation.
- All resistors are utilized are of premium quality with a 1% tolerance.
- This tiltmeter was hand-assembled, calibrated, and tested at the plant with stringent quality control standards from the manufacturer.
- The temperature sensor that is installed in the base and allows users to record and evaluate the effects of temperature changes on measured structural and ground behavior.

The use of the tiltmeter is required, as in a previous study done by [Anna], a correction factor to the value of the gravity must be taken into account due to the inclination of the surface where it is placed. In the previous research done with the same equipment, a correction factor shown on equation 11 is

$$\delta_g(nms^{-2}) = g (1 - \cos \theta) \cong 5 * 10^{-3} \theta^2 (\mu rad) \quad (10)$$

Where the function of the inclination, $\theta(t)$, was obtained by the tiltmeter.

b) Technical specifications of the tiltmeter

The following list specifies specifications of the tiltmeter model 714 from Applied Geomechanics (Applied Geomechanics).

- Angular Range: ± 8000 μ radians
- Uncertainty: ± 0.46 degree
- Scale factor: 1 μ radian/mV
- Resolution: 0.1 μ radian
- Repeatability: 1 μ radian
- Linearity: 2% of full span
- Temperature coefficient
 - Scale factor: $KS = +0.05\%/^{\circ}C$ typ
 - Zero shift: $KZ = \pm 3$ μ radians/ $^{\circ}C$ typ
- Tilt output: ± 16 Volts DC (differential)
- Output impedance: 270 Ohms
- Temperature operation range: -25° to $+70^{\circ}$ C
- Temperature output:

- Scale factor: $0.1^{\circ}\text{C}/\text{mV}$ (single-ended)
- Operation range: -40° to $+100^{\circ}\text{C}$,
- Accuracy: $\pm 0.75^{\circ}\text{C}$ accuracy
- Zero point: $0^{\circ}\text{C} = 0 \text{ mV}$

C. Agilent 34970A Data Acquisition / Switching Unit

The Agilent 34970A data acquisition and switching unit is an extremely powerful acquisition system that has several features and has a high versatility of operations. It can be used for the monitoring of up to 20x3 channels both in DC and AC as well as options to monitor thermocouple, thermistor and RTD temperature measurements. It can be used as a voltage source both in AC and DC and it has 3 expansion slots with 8 different expansion cards utilized for several diverse applications (Agilent).



Figure 17. Agilent 34970A Data Acquisition / Switching Unit

a) *Technical Features*

The main technical features of the switching unit are listed below (Agilent).

- Scanning of up to 120 analog input channels
- Measurements of AC and DC signals

- Capability to monitor temperature instruments such as thermocouples, thermistors and RTD's
- Capability to measure, 2 and 4 wire resistance
- Capability to measure AC and DC currents.
- Capability to monitor frequency, and period of AC signals
- 6.5 digits of resolution (22 bits) with 0.004% accuracy for DC voltages
- 50k reading nonvolatile memory including timestamp
- Scaling and alarms available on each channel
- Scan rates up to 250 channels per second
- GPIB and 115 kbaud RS-232 interfaces standard
- Software drivers available for Agilent VEE and National-Instruments LabView

The basic requirements for this gravitational station where that the acquisition system allows for a minimum of 8 channel monitoring systems with a space for growth for future implementation of sensors and the possibility to connect it to a computer to control the data acquisition and for manipulation and storage of the received data. Lastly, as for every acquisition system, the highest possible resolution of the acquisition system was valuable, as the gravitational measurements due to tidal fluctuations are extremely small, and a high resolution could allow for a better detection of them. As shown by the technical characteristics, the Agilent 34970A switching unit is capable of monitoring up to a 22 bit resolution, 6.5 significant figures with an accuracy of 0.04% and proves to accomplish all these requirements, making it a perfect candidate for this application (Agilent).

b) Channel Delay Characterization

One important parameter to determine from the Agilent 34970A data acquisition and switching unit was the time delay it takes from the measuring of one channel to the next channel. It should be noted that for gravimetric applications, timing is an extremely important parameter as the synchronization of different gravimetric stations is utilized for several research projects. Therefore, reporting the delay that this device will take between the measure of each channel, and evaluating its effect on the entire system is vital.

On the hardware side, on the back of the switching unit there is space for three expansion slots. This is shown on the following picture:



Figure 18. Agilent 34970A Data Acquisition / Switching Unit Backside

On the upper slot, a 20-channel general purpose switch was introduced. This allows for the switching unit to be able to measure 20 different channels. An example of this expansion card and its connections is shown on the images below:

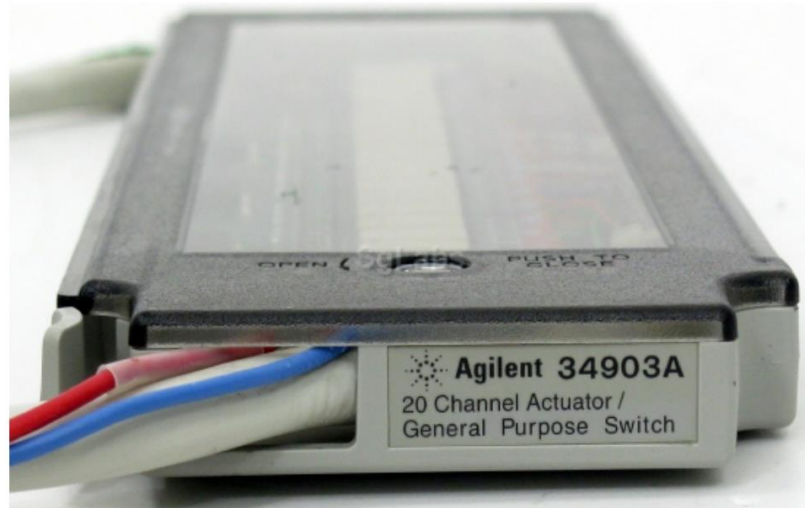


Figure 19. Channel Expansion Card Side View



Figure 20. Channel Expansion Card Top View

With a function generator, a sinusoidal with a frequency of 1Hz and an amplitude of 3V was generated and the same was introduced on the first 8 channels of the acquisition unit. Then with LabView, utilizing the SCPI command language for the Keysight 34970A data acquisition system (Keysight), a directive to measure the same signal on the 4 channels was sent. This process and the SCPI directives will be further explained on the software section below. In theory, by sending measuring directive at the same time for the first 4 channels which are connected to the same signal, all the channels should measure the same value of the generated sinusoidal. However, as shown on the graph below, the sinusoidal from each channel shows an apparent small phase shift compared to the ones of the previous channels.

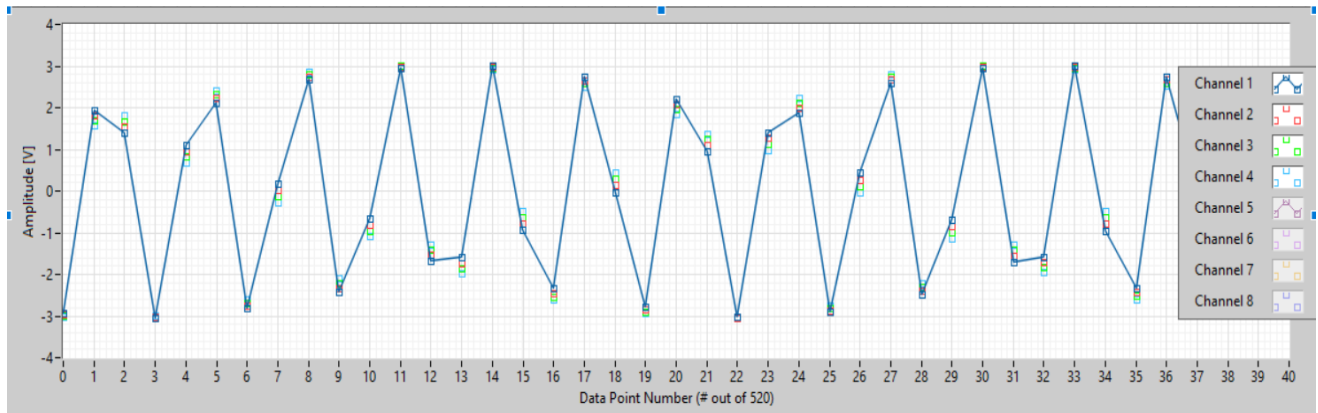


Figure 21. Data acquired from the first 4 Channels

This problem was further amplified as more channels were introduced on the scanning list. To scan several channels, a scanning list should be first specified with the following SCPI command:

- `rout:scan (@101,102,103,104)`

This command will scan the first four channels on the expansion card inserted into the switching unit. However, as the list increases further than 6 channels, the switching unit is not able to process the whole scan list as it exceeds the memory limitations for a single scan. Therefore, to scan more than 6 channels, two different scan lists should be established. To scan 8 channels, the SCPI directives should be

- `rout:scan (@101,102,103,104)`
- `rout:scan (@105,106,107,108)`

The set up of the scanning lists will introduce an additional delay between channel number 4 and channel number 5, and also between channel number 8 and channel number 1 as the channel list should be reset to the original scanning list to acquire data from the first four channels. Graphically, this can be seen as a larger phase shift between the first four channels and the

posterior four channels. This can be seen on the following graph, where the first four channels seem to have a small faze shift among each other, but they have a larger apparent faze shift with the following four channels.

On Figure 22, channel 1 is graphed in blue, while channel 5 is graphed in purple, showing an apparent faze shift between the signals (Keysight),.

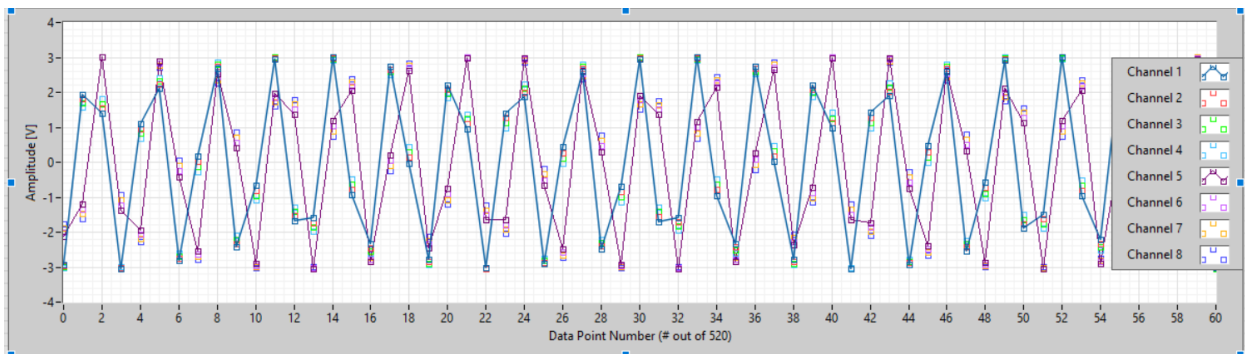


Figure 22. Data Acquired from 8 Channels

This process of switching between channel lists for the measurement of 8 channels was done a total of 520 times to gather a large data set of points.

To calculate the delay between the channels, the inverse function of the sinusoidal was utilized to determinate the apparent time at which each measurement was taken. Knowing the direct function of the sinusoidal:

$$y = A * \sin(2\pi ft)$$

Where the amplitude of the signal was $A = 3V$ and the frequency $f = 1Hz$, the inverse sinusoidal function is to determine the apparent time at which the measurement was done is:

$$t = \frac{1}{2\pi f} \sin^{-1} \left(\frac{y}{A} \right)$$

Finally, by repeating this procedure for each datapoint obtained on each channel, a list of times: t_{CH1} through t_{CH8} was achieved for the where the diverse measurements each of the 8 channels.

To determinate the delay between the measurements between channels 1 and 2, equation 13 was implemented:

$$delay_{CH1-CH2} = |t_2 - t_1|$$

Generalizing for any channel I on equation 14. :

$$delay_{CHi-CHi+1} = |t_{i+1} - t_i|$$

Note that the absolute value is required as the inverse sine function has negative values between the values of -1 and 0. With these considerations, the following delays between channels were obtained and are presented on Table 3.

Delay Between Channels			Delay [s]	Standard Deviation [s]
1	&	2	0.00832	0.00088
2	&	3	0.00792	0.00089
3	&	4	0.00770	0.00086
4	&	5	0.12357	0.04000
5	&	6	0.00827	0.00094
6	&	7	0.00798	0.00103
7	&	8	0.00777	0.00777
8	&	1	0.15605	0.05876

Table 3. Channel Delay Results

As it can be seen from the table above, channels on the same scanning list have a low delay between each other. However, when the scanning list must undergo a reset and change, the delay is increased considerably. Finally, separating the delay of the channels that are on the same scanning lists, from the delay of channels between scanning lists and averaging them, the expected delay between channels is the following:

Between subsequent channels on the scanning list:

- Expected delay: 7.99ms
- Standard variation: 2.06ms

Between channels on different scanning lists:

- Expected delay: 140.0ms
- Standard variation: 49.4ms

With the delay values, a couple of observations must be noted.

- Variables of higher importance and with a higher variability over time should be prioritized and placed on the lowest possible channels as the delay accumulates from channel to channel.
- Variables that influence other variables should be placed on subsequent channels and splitting them into different channel lists should be avoided. For example, the inclination is utilized to correct the gravimetrical acceleration, so they should go on subsequent channels, preferably on the first scanning list.
- Variables with a lower dynamic nature, such as temperature or the voltage supply can be placed on higher channels.
- Finally, as studied on (A. Albano, 2015) the frequency at which gravitational metrological node takes its measurements is 0.2Hz, I.e. a sampling period of 5 s. Therefore, a delay of 7.99ms for subsequent channels and 140.0 on between channel lists represents a 0.16% and 2.8% respectively compared to the 5 second sampling period. In comparison, the delay values are extremely low, therefore for this particular application the order of the measurement does not have such an important effect on the measurements. However, in another application where signals that are measured with a higher frequency, the previous mitigation actions should be taken into account to avoid delay issues.

D. Other equipment

The final hardware elements required for the gravitational station where a voltage supply for the tiltmeter and a computer for the measurement control, data processing and storage. In terms of the power supply, the only requirement was that it can maintain a constant voltage of

+12V and -12V for long periods of time without variations. In particular, the model Codevintec Model 02-4380 was chosen as it accomplished this requirement.

In terms of the computer, the only requirement was that it was able to run a version of LabView that allows for the NI-VISA drivers, as included in them is the GPIB 488.2 functions pallet which is utilized for the bilateral communication with the Agilent data acquisition and switching unit. However, these packages have support for LabView since versions dating back to 2014 and supported in operating systems that go back to Windows XP. Therefore, the requirements for the computer on the hardware side for the metrological station was not difficult to accomplish. For this project, a computer with an Intel Xeon XE, 4GB of RAM, with a 200GB SSD, running Windows XP and LabView version 14.0 surpassed the requirements for the gravitational station.

All the hardware sensors of the system are shown on the photo of figure 23.



Figure 23. Sensors of Gravitational Station

In the upper left corner, the tiltmeter is shown. On the lower left corner, the gravimeter is located. Connected to the gravimeter, in the middle, the voltage supply control for the gravimeter is located. The gray box controls the voltage supply that is utilized to power the gravimeter. It has a control system that takes energy out of the electrical grid and powers both the gravimeter and the battery, which is located on the right side of the image. The control box switches the energy supply for the gravimeter between the electrical grid and the battery so that the gravimeter in case the system is disconnected from the energy supply. This is fundamental as a disconnection of the gravimeter from the power grid for long periods of time as this might lead to a decrease of the internal temperature of the gravimeter which will affect the correct operation of the device.

On the figure 24, the computer where the data is being processed as well as stored can be observed. On the right-hand side of the table, in the back the voltage supply for the tiltmeter is located. On the bottom right-hand side of the table, the Agilent Switching unit is located.

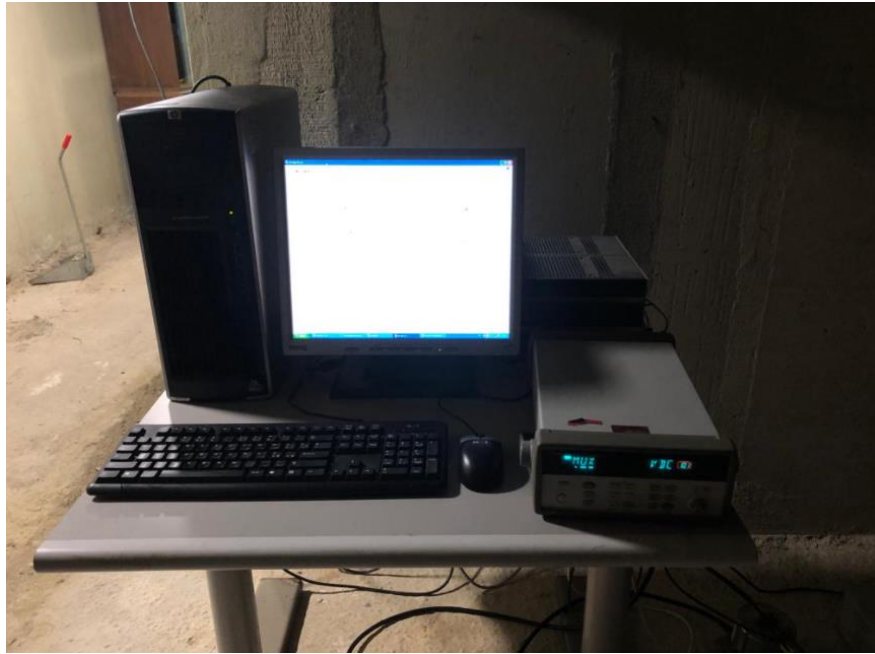


Figure 24. Computer, Power Supply and Acquisition Unit.

Lastly, as the images show, the metrological station is located on a secluded area. This is an advantage as the sensors will not be disturbed by bystanders passing by. Now that the hardware section of the metrological station is being fully described, is time to explain the software side of the station.

2. Software Implementation

For the software implementation, a program was created in LabView for the control and acquisition of the geological parameters studied on this metrological station. On the front end, figure 25, the running program is minimal:

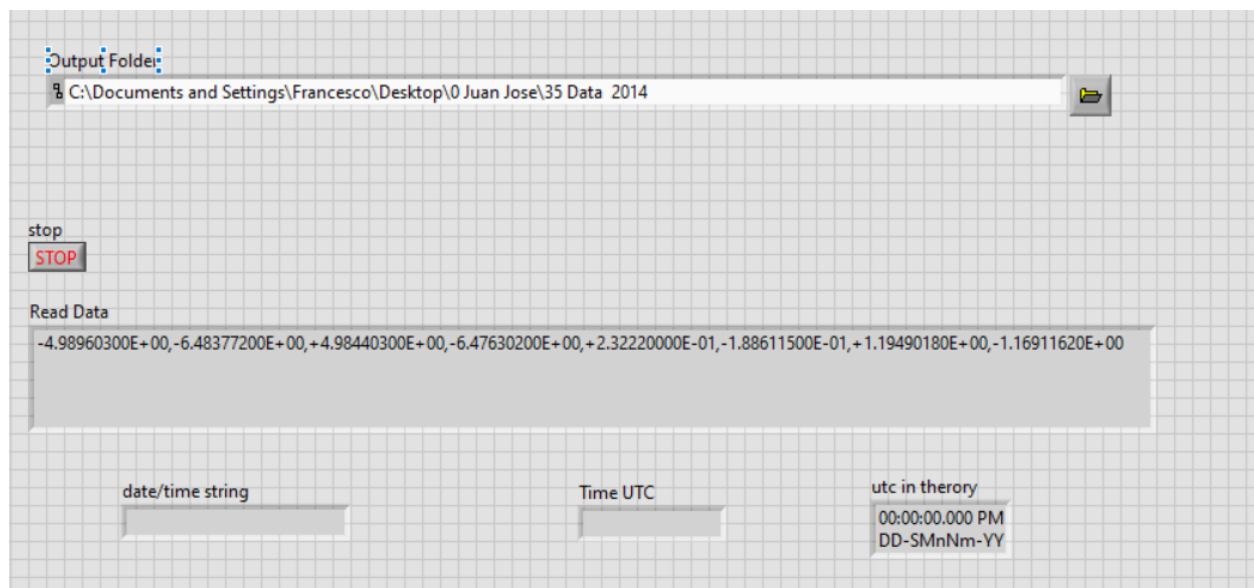


Figure 25. LabVIEW Front End Interface

From top to bottom, it contains a folder path where the data that is being processed is being saved, as well as indicators for the last read data, an indicator for the date and time in string format which shows the date and hour that the data was taken, and lastly, an indicator of the date and hour in UTC format, which is how the information is presented on gravimetical studies.

On figure 26 the back end the following panel is shown:

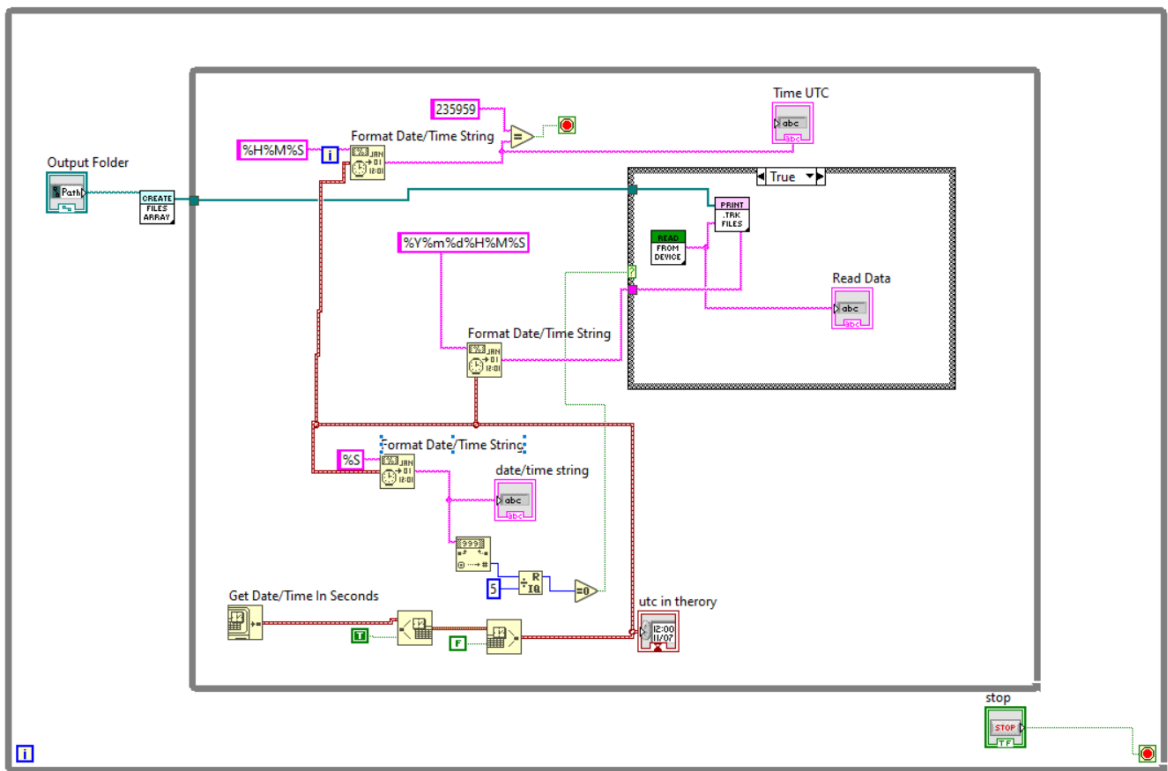


Figure 26. LabVIEW Backend View

As we can see, there is a diversity of modules that have a desired action. Each one of them will be detailed in the following sections.

A. File Creation Block:

Starting from the left of the back-end panel, the create files SubVI:

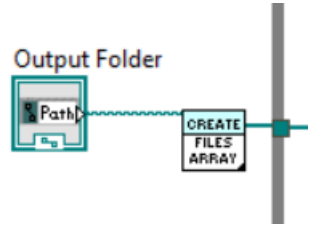


Figure 27. Create Files SubVI Icon.

When opening this block, the logic for the creation of the files is found. In the beginning, the following panel is found on figures 29-30:

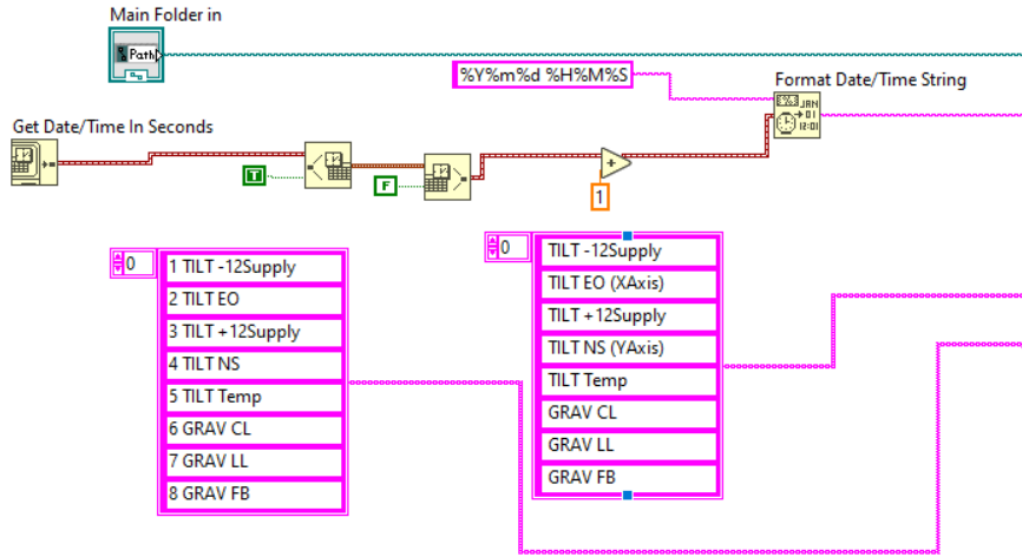


Figure 28. Create Files SubVI pt1.

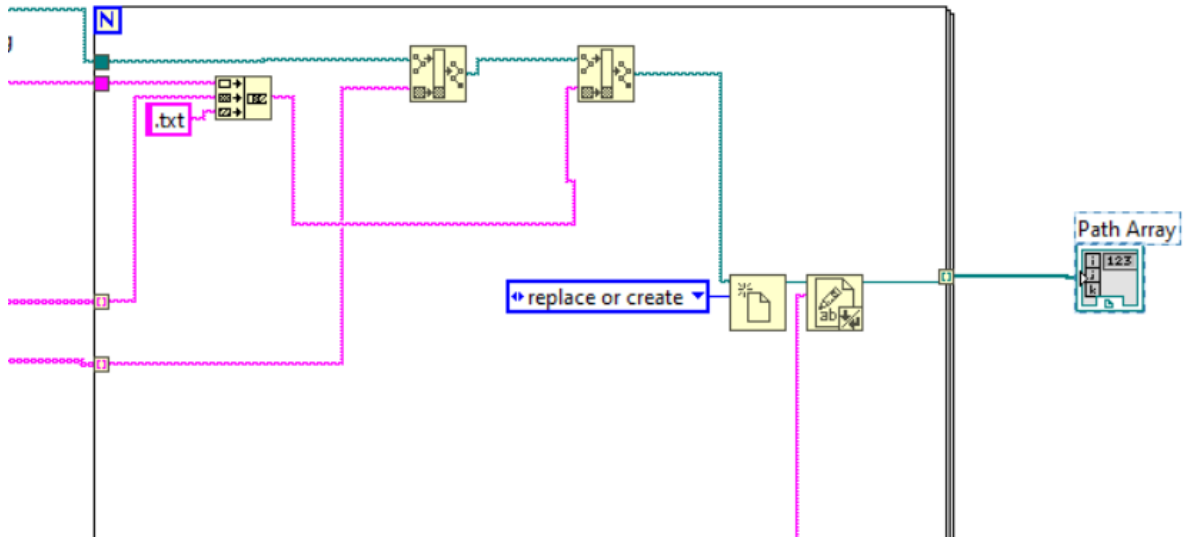


Figure 29. Create Files SubVI pt2.

In the top corner, the main folder path where the data reports are being saved is passed to the next section. On the second row, an initial “Get Date/Time in Seconds” block is being placed, and then the time is transformed into UTC format. The process of the creation of the different files is done every-day at 23:59:59. That is why an addition of 1 second is done so that the name

of the file is created with the date of the next day. This is done 1 second before the next day so that it does not interrupt the data acquisition process.

The next two array of strings include: at the left the folder name where the data will be stored so that every variable is saved on its own folder, and the second one includes the initial part of the name that the file will take. The second part of the name that the file will take will include the date and the hour that the file was created, obtained at the end of the second column. By doing this, all the files will have on the name: the indicator of what parameter the file is measuring, the date that the data was taken, and lastly the hour of the creation of the file. Since the data is separated in different files for every day and the creation of the data is done at 23:59:59 plus 1 second, the hour of the creation of the file will always be 000000 (hour format without the : character). This is also a safety feature in case the acquisition system is stopped during the day, as an overwrite of the data is undesired, and it will be easier to merge the files afterwards. The second image shows how the strings are combined for the creation of each of the individual text files, and lastly, the output of this block is an array with the path of the created files will be used later for the writing of the data into the .txt files.

For example, the file named “20220111 000000 GRAV FB.txt” corresponds to the gravimeter feedback channel, corresponds to the 11th of January of 2022 and was correctly created at midnight. Moreover, this file will be located on the “<MainFolder>\8 GRAV FB\” directory along with the other files for the gravity feedback channel acquired on different days.

Figure 30 of the File Creation Block SubVI contains the following blocks:

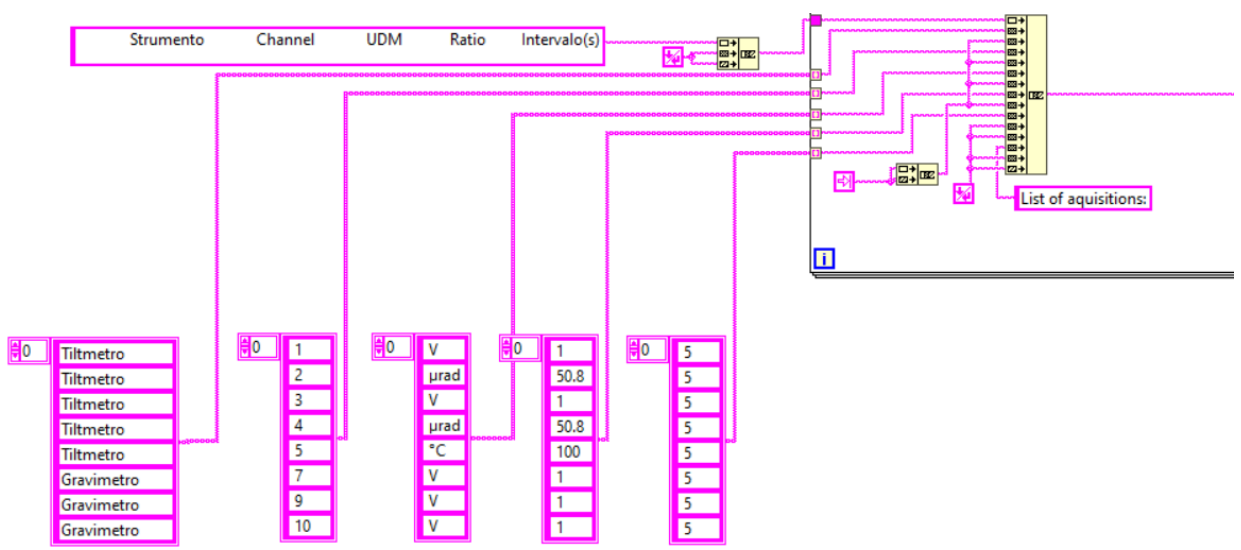


Figure 30. Create Files SubVI pt3.

This section only makes sure to correctly print a header for each of the 8 files generated of the 8 different parameters that are being studied by the gravimeter or tiltmeter. This header includes the instrument where the information was taken on, the channel to which is connected on the Agilent Switching unit, the unit of measurement of that particular parameter, the ratio to transform between that unit of measurement from the input voltage signal, and lastly, the interval in seconds which separates the different measurements of that quantity. For the previous example of the “20220111 000000 GRAV FB.txt” file, the header on this file will be the following. On this case, the unit of measurement is the volt and there is no transformation into an acceleration since that should be done further by specialists that will utilize this information and will use their models to determinate the gravity. In the meantime, this file only reports the raw data obtained as a voltage signal. That is why the conversion ratio is 1 as shown of figure 32.

1	Strumento	Channel	UDM	Ratio	Intervalo (s)
2					
3	Gravimetro	10	V	1	5
4					
5	List of aquisitions:				
6					
7	20220111000000			1.234522E+0	
8	20220111000005			1.234160E+0	
9	20220111000010			1.240968E+0	
10	20220111000015			1.278922E+0	

Figure 31. Header Example of .txt

B. Time Based Control Structures

In the main back-end diagram, figure 32, the hour is utilized on several instances in order to control the two while loops utilized and the case structure. At the beginning, date and time are obtained and transformed into UTC format with the following blocks.

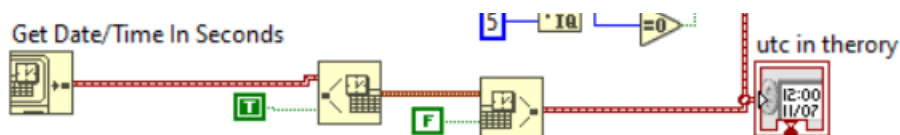


Figure 32. UTC Time Transformation

Once the hour is in UTC time, it is used for several internal controls. In the control of figure 33:

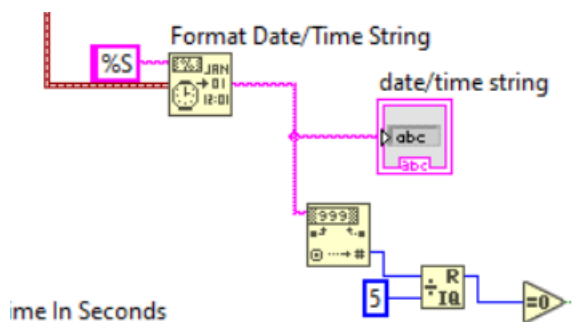


Figure 33. Condition for 5 sec Acquisition

From the data in UTC, the seconds information is extracted into a string. That string is then transformed into an integer number and an integer division by 5 is performed. If the result is 0, it

means that the second where this is a multiple of 5 and makes the actions inside the case structure execute. These actions will be discussed in the following section.

In the second control, figure 34, the signal that is obtained with the UTC hour is transformed into a string and an evaluation of the time is done

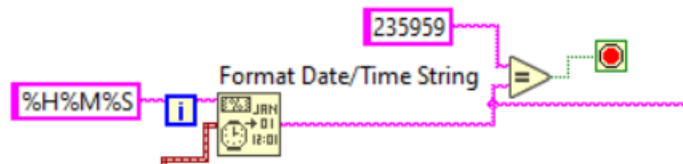


Figure 34. Condition for New File Creation

The output of the equality will acquire a true value only if the current time (in UTC) is equal to 23:59:59. If this condition is met, the internal while loop will be stopped, and the external while loop will come into action. The external file creation block is the one in charge of the creation of the files discussed on the previous section.

Lastly, the UTC date and hour information is formatted so that the date and hour enter the true condition of the case block. It should be noted again that the true condition of this block is accessed only at multiples of 5 seconds starting at midnight every day. The False condition of the case block is completely empty. On the true condition, two different actions are taken place as shown on figure 35:

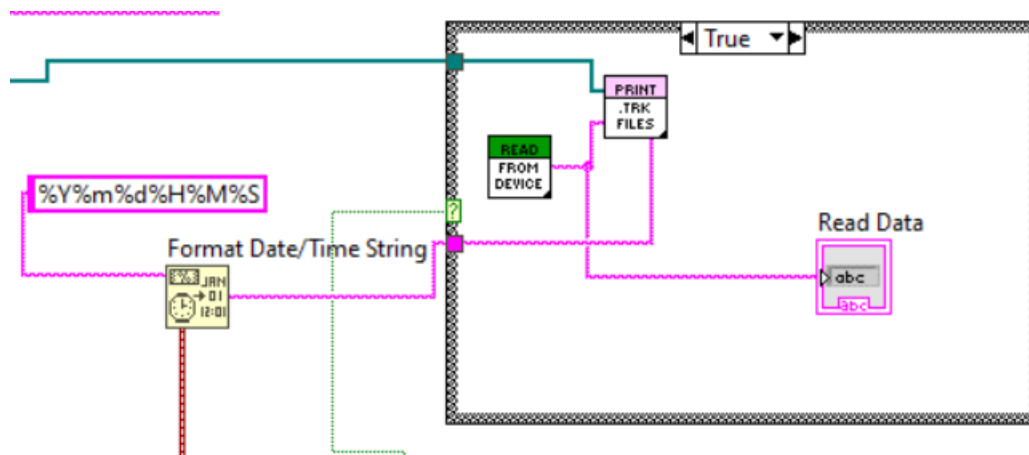


Figure 35. Reading and Writing Data

The two actions that are taken inside of this block are the following: reading from the device (green block) and printing the different .txt files (pink block). These blocks contain Sub VI's that will be further explained on the following sections.

C. Read From Device:

The read from device Sub VI oversees the bilateral communication with the Agilent 34970A Data Acquisition & Switching Unit. They are connected by a USB to RS-232 cable that connects the computer with the acquisition system in that order. Then, by directives utilizing the SCPI command language and utilizing the GPIB send and receive modules from the GPIB 488.2 function library the communication between these two devices is achieved.

The scanning of the channels of the different channels requires the individual configuration of them. In the configuration, the maximum amplitude expected must be inserted as well as the resolution expected on the reading. To scan the eight channels of that the gravitational station has, a higher emphasis was done on separating the channels based on the expected operating range, and signals were grouped based on the maximum values that they can achieve. By doing this, three different scanning lists were set. The first one scans the variations

of the inclination signals of the tiltmeter as well as its voltage supply and is set to measure up to 20V. The second one oversees measuring the temperature obtained by the tiltmeter, measuring up to 5V. Lastly, the last scanning list contains the values of the gravimeter and is set up to measure up to 10V.

The following commands SCPI directives were implemented in order to scan the 8 channels currently evaluated, and the process is repeated every 5 seconds. The commands are the following

- *rst
- conf:volt:dc 20,0.0001, (@101,102,103,104)
- rout:scan (@101,102,103,104)
- init
- fetch?
- conf:volt:dc 5,0.0001, (@105)
- rout:scan (@105)
- init
- fetch?
- conf:volt:dc 10,0.0001, (@107,109,110)
- rout:scan (@107,109,110)
- init
- fetch?

The block diagram that communicates the previously stated directives are shown on figure 36 and 37.

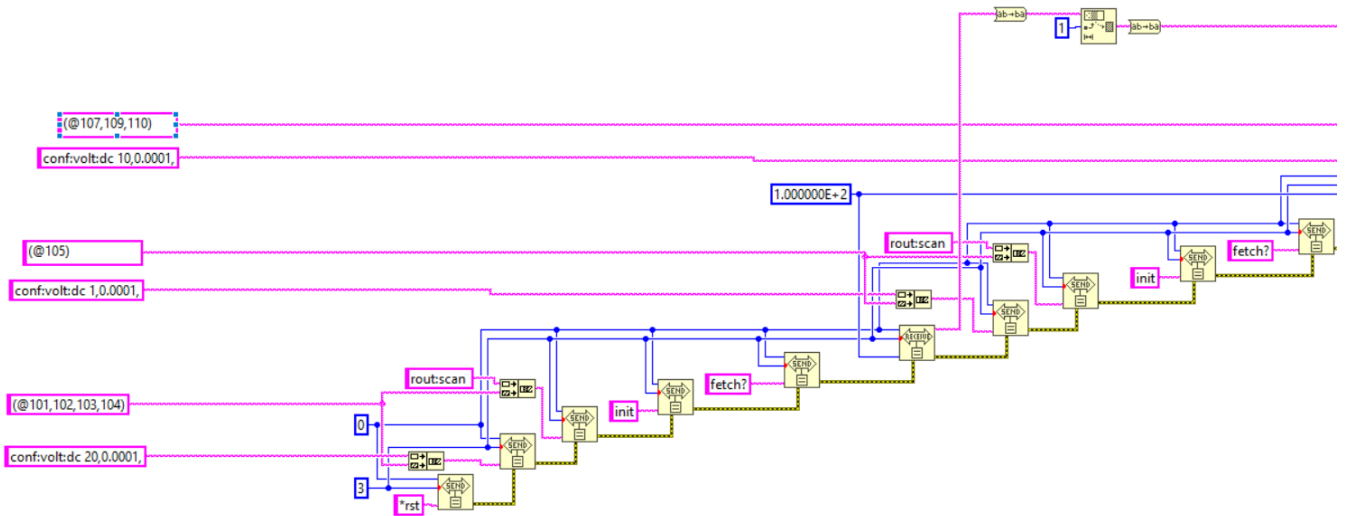


Figure 36. Communication with Switching unit pt1.

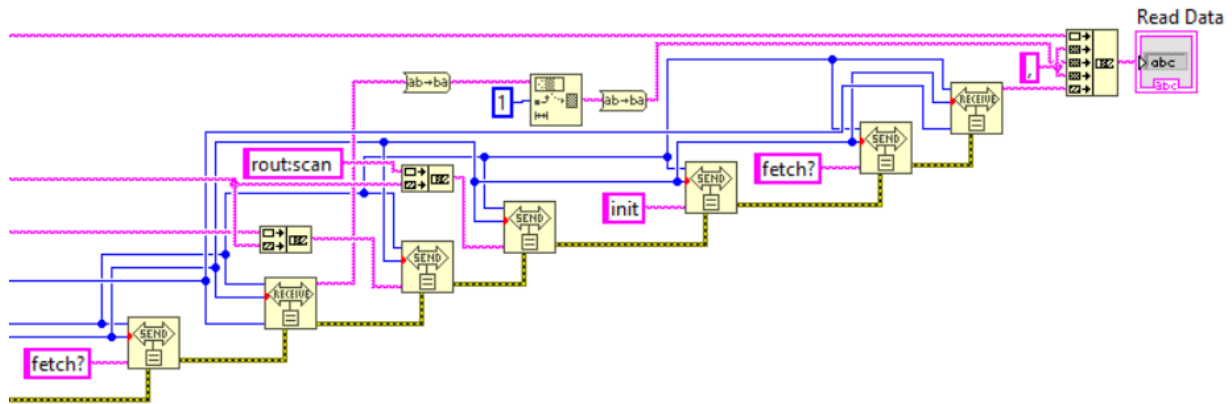


Figure 37. Communication with Switching unit pt2.

It should be noted that in the upper lines, blocks were introduced to eliminate the new line creation after each of the reading directives, and at the end, commas were introduced to

maintain the data obtained by different channels separated by commas. In this way, the final read data will take the following shape:

$-4.98960300E+00,-6.48377200E+00,+4.98440300E+00,-6.47630200E+00,+2.32220000E-01,-1.88611500E-01,+1.19490180E+00,-1.16911620E+00$

Where the eight measurements of the different channels are presented in scientific notation, with the dot (.) as a decimal separator and the comma (,) as a separator for the different measurements. The next block will separate the data, process it and print it into the different .txt files created on the file creation block.

D. Write into .txt SubVI

The final block is in charge of printing the different measurements on the correct .txt files from each of the parameters that is being measured. The block diagram of this Sub VI is shown on figure 38:

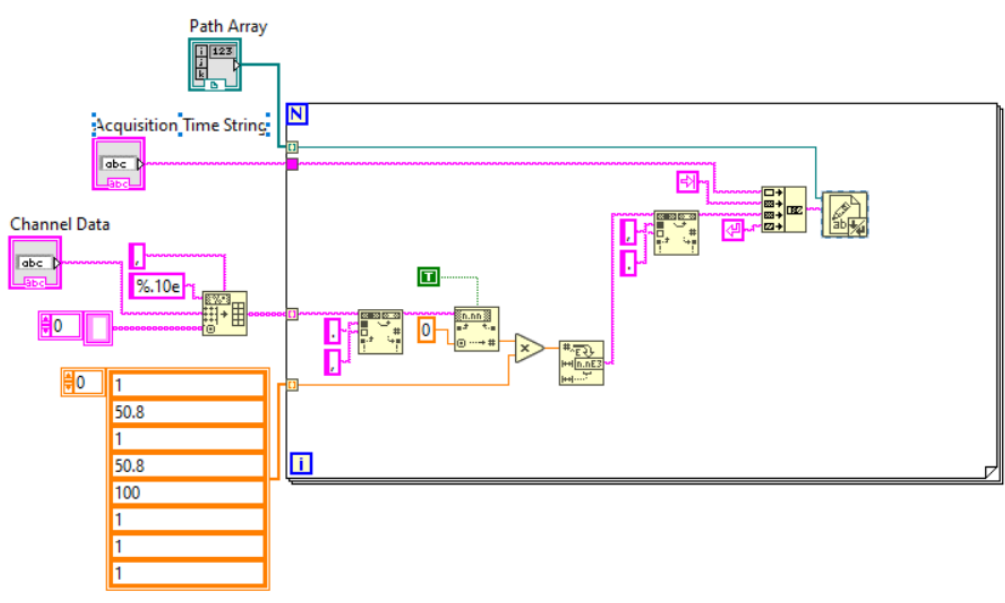


Figure 38. Write into .txt SubVI.

As an input, this block has the path array where the locations of the diverse .txt files are located. An acquisition time string that includes the date and the time that the measurement is also passed into the block, as when the data is printed, a time stamp that indicates this information will be placed before the measured data. The channel data first separated into an array and then converted into a double variable. This is done in order to multiply the values by the transformation ratios that will change the voltage signal into the correct measured parameters. In this case, the measured parameters that are transformed are the inclination of obtained by the tiltmeter that is transformed by multiplying it by a factor of $50.8\mu\text{rads/V}$. In the same way, the temperature value is multiplied by a scaling factor of 100°C/V . The other measurements remain in volts, as the researchers that utilize this information will utilize diverse methods and models to finally transform the electrical signals into the desired parameters.

Finally, the numerical values of the diverse measurements are further transformed back into a string type character, it is joined with the time stamp that indicates the time at which the measurement was done and finally, with the write to txt block, the data is written in the corresponding .txt file.

CHAPTER 3: RESULTS

1. Folder Structure and graphs:

Figure 39 shows the Main Directory where the data is stored of the 8 channels monitored through the months of January and February of 2022:

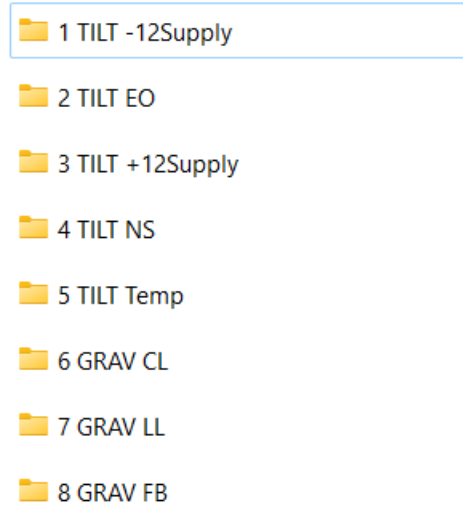


Figure 39. File Organization

Each folder is filled with data separated every day based on UTC standard time and separated on daily files as on figure 40.

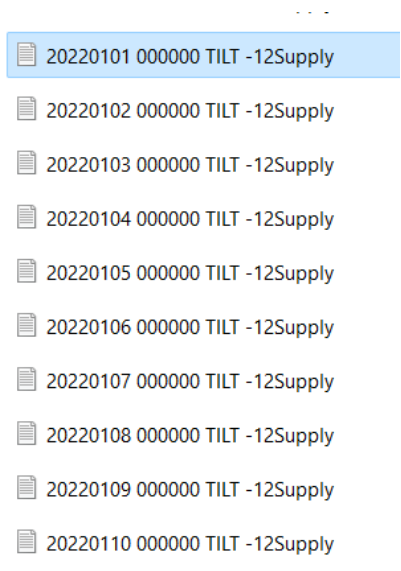


Figure 40 Folder File's Example

Figures 41-48 show examples of each type of file gathered, its decimal precision, the unit

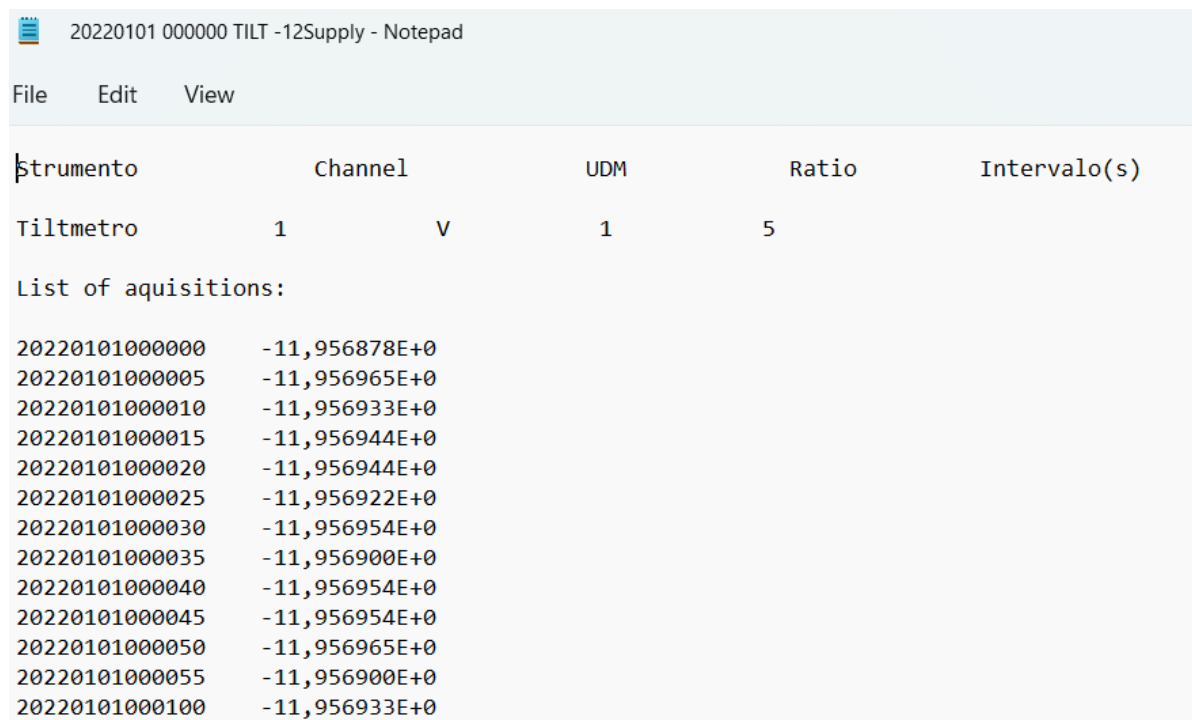


Figure 41. -12V Channel monitoring example

20220101 000000 TILT +12Supply - Notepad

File Edit View

Strumento	Channel	UDM	Ratio	Intervalo(s)
Tiltmetro	3 V	1	5	

List of aquisitions:

20220101000000	12,008106E+0
20220101000005	12,008160E+0
20220101000010	12,008138E+0
20220101000015	12,008149E+0
20220101000020	12,008149E+0
20220101000025	12,008149E+0
20220101000030	12,008149E+0
20220101000035	12,008138E+0
20220101000040	12,008138E+0
20220101000045	12,008171E+0
20220101000050	12,008149E+0
20220101000055	12,008128E+0
20220101000100	12,008117E+0

Figure 42. +12V Channel monitoring example

20220101 000000 TILT EO (XAxis) - Notepad

File Edit View

Strumento	Channel	UDM	Ratio	Intervalo(s)
Tiltmetro	2 μ rad	50.8	5	

List of aquisitions:

20220101000000	-986,282102E+0
20220101000005	-986,281035E+0
20220101000010	-986,279917E+0
20220101000015	-986,282102E+0
20220101000020	-986,278800E+0
20220101000025	-986,281543E+0
20220101000030	-986,281035E+0
20220101000035	-986,279917E+0
20220101000040	-986,278800E+0
20220101000045	-986,279917E+0
20220101000050	-986,281035E+0
20220101000055	-986,279358E+0
20220101000100	-986,278241E+0

Figure 43. Tiltmeter EW Channel monitoring example

20220101 000000 TILT NS (YAxis) - Notepad

File Edit View

Strumento	Channel	UDM	Ratio	Intervalo(s)
Tiltmetro	4 μrad	50.8	5	

List of acquisitions:

20220101000000	-985,811490E+0
20220101000005	-985,811490E+0
20220101000010	-985,811490E+0
20220101000015	-985,811490E+0
20220101000020	-985,810932E+0
20220101000025	-985,810932E+0
20220101000030	-985,809865E+0
20220101000035	-985,812608E+0
20220101000040	-985,809865E+0
20220101000045	-985,810424E+0
20220101000050	-985,809865E+0
20220101000055	-985,809865E+0
20220101000100	-985,809306E+0

Figure 44. Tiltmeter NS Channel monitoring example

20220101 000000 TILT Temp - Notepad

File Edit View

Strumento	Channel	UDM	Ratio	Intervalo(s)
Tiltmetro	5 $^{\circ}\text{C}$	100	5	

List of acquisitions:

20220101000000	15,190000E+0
20220101000005	15,179000E+0
20220101000010	15,179000E+0
20220101000015	15,179000E+0
20220101000020	15,173000E+0
20220101000025	15,173000E+0
20220101000030	15,173000E+0
20220101000035	15,184000E+0
20220101000040	15,179000E+0
20220101000045	15,184000E+0
20220101000050	15,168000E+0
20220101000055	15,190000E+0
20220101000100	15,184000E+0

Figure 45. Temperature Channel monitoring example

20220101 000000 GRAV CL - Notepad

File Edit View

Strumento	Channel	UDM	Ratio	Intervalo(s)
Gravimetro	7 V	1	5	

List of aquisitions:

20220101000000	-732,137200E-3
20220101000005	-731,992300E-3
20220101000010	-731,992300E-3
20220101000015	-732,137200E-3
20220101000020	-732,064800E-3
20220101000025	-731,992300E-3
20220101000030	-732,064800E-3
20220101000035	-732,354500E-3
20220101000040	-732,137200E-3
20220101000045	-732,137200E-3
20220101000050	-732,354500E-3
20220101000055	-732,064800E-3
20220101000100	-731,919900E-3

Figure 46. Central Level Channel Monitoring Example

20220101 000000 GRAV LL - Notepad

File Edit View

Strumento	Channel	UDM	Ratio	Intervalo(s)
Gravimetro	9 V	1	5	

List of aquisitions:

20220101000000	-391,636900E-3
20220101000005	-446,540000E-3
20220101000010	251,264700E-3
20220101000015	310,368800E-3
20220101000020	-20,570500E-3
20220101000025	-46,863200E-3
20220101000030	-301,821900E-3
20220101000035	283,134600E-3
20220101000040	-317,394700E-3
20220101000045	325,651800E-3
20220101000050	32,087100E-3
20220101000055	302,691100E-3
20220101000100	277,991900E-3
20220101000105	212,876100E-3
20220101000110	257,856000E-3

Figure 47. Lateral Level Channel Monitoring Example

20220101 000000 GRAV FB - Notepad

File Edit View

Instrumento	Channel	UDM	Ratio	Intervalo(s)
Gravimetro	10	V	1	5

List of acquisitions:

20220101000000	1,467534E+0
20220101000005	1,458770E+0
20220101000010	1,457031E+0
20220101000015	1,455728E+0
20220101000020	1,467244E+0
20220101000025	1,457031E+0
20220101000030	1,468910E+0
20220101000035	1,452033E+0
20220101000040	1,450295E+0
20220101000045	1,466592E+0
20220101000050	1,451237E+0
20220101000055	1,445297E+0
20220101000100	1,459494E+0

Figure 48. Feedback Channel Monitoring Example

2. Gravimetric Monitoring

As the main parameter of study of interest for gravitational applications is the gravity, the raw data obtained during January and February of 2022 is presented on figure 49:

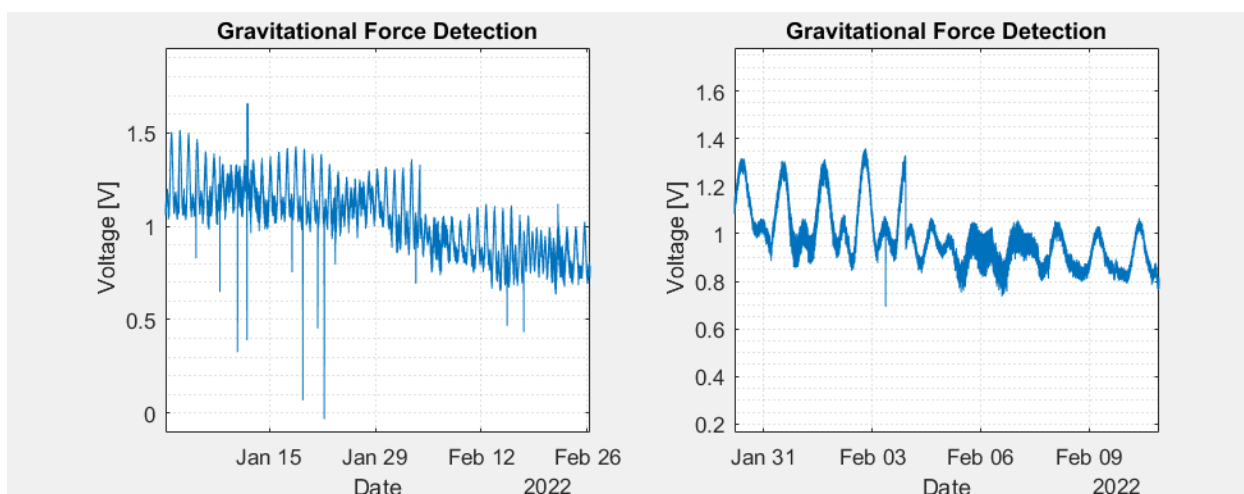


Figure 49. Gravitational Acceleration Raw data of January and February 2022

As it can be seen on the right side of picture where only 3 days are analyzed, the signal follows a period of approximately 24 hours with two pics. Further research on this variation show to correspond to the tidal variations due to tidal changes on the ocean. Therefore, the collected data can be used on further research on investigations that require this data. To additionally complement this information, other metrological data is also presented.

Figure 50 and 51 present the inclination on both of earth's axis and its variation on the studied period, since as shown on (A. Albano, 2015), this information can be further while processing the data to increase the accuracy of the measurements.

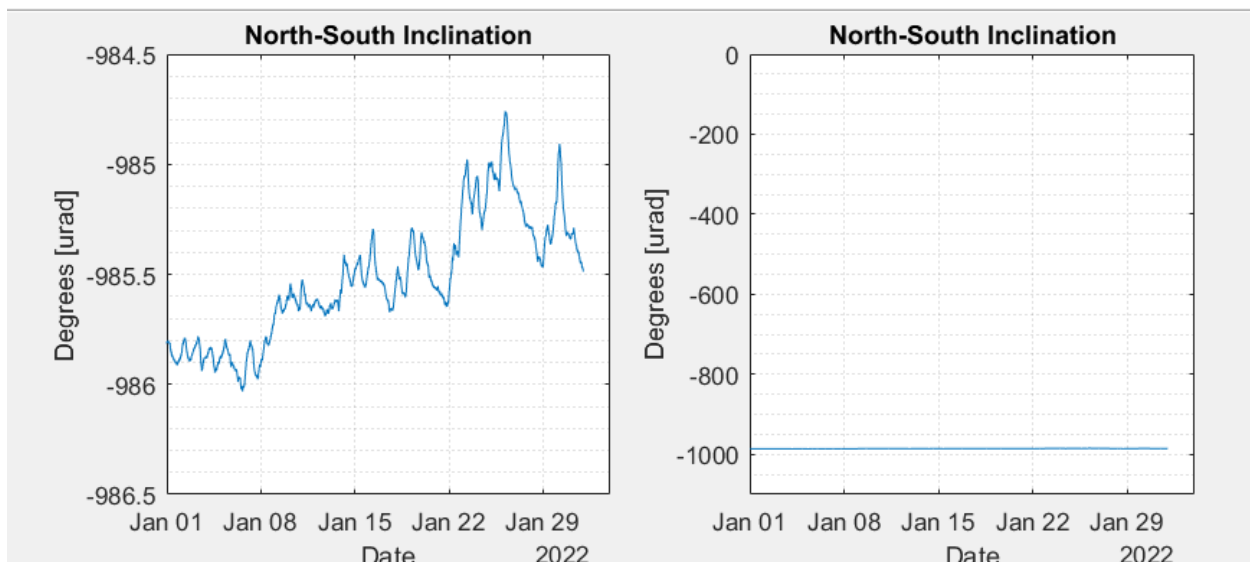


Figure 50. Inclination of North-South Axis

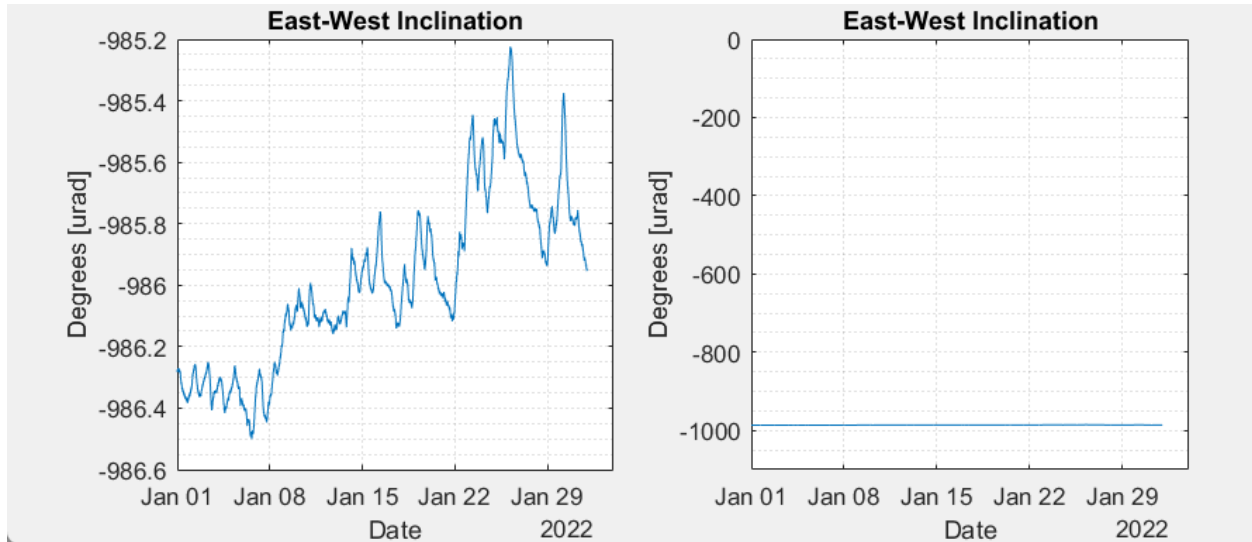


Figure 51. Inclination of East West Axis

In particular the expected effect of inclinations on the gravimetric studies in (A. Albano, 2015), is shown on equation 17:

$$\begin{aligned} \delta_g [nms^{-2}] &= g (1 - \cos \theta) \\ &\cong 5 \cdot 10^{-3} [\mu rad] \end{aligned} \quad (15)$$

Additionally, other metrological station located in the same university as this project is researched, Università della Calabria in Arcavacata, Cosenza, also provides additional metrological parameters. Noted that this station is within a 400m distance of our location site and are shown figures 52 and 53.

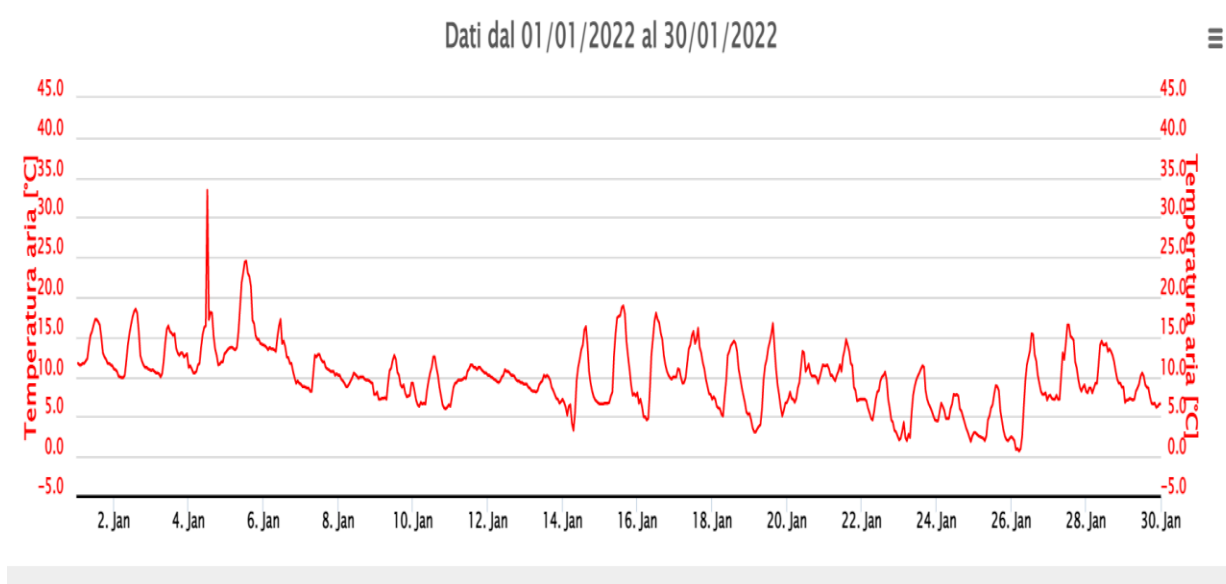


Figure 52. Temperature Monitoring for January 2022

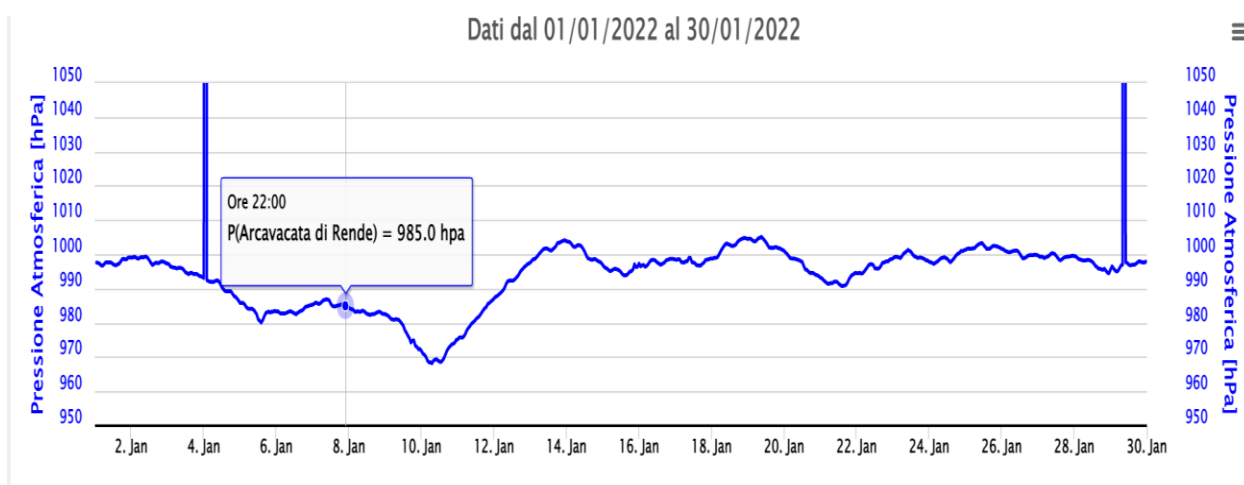


Figure 53. Pressure Monitoring for January 2022

It is also mentioned in (A. Albano, 2015), that the pressure might introduce additional uncertainty in the order of:

- -2.9 ± 0.2 [$\text{nm s}^{-2} \text{hPa}^{-1}$].

While temperature might introduce additional uncertainty in the angle of inclination in the order of the direction (A. Albano, 2015):

- 5.28 ± 0.03 (E-W) [$\mu\text{rad}/^\circ\text{C}$]
- 1.94 ± 0.05 (N-S) [$\mu\text{rad}/^\circ\text{C}$]

3. Additional Measured Parameters:

Additionally, the electronic level channels obtained from the gravimeter are also presented on figure 54 and 55.

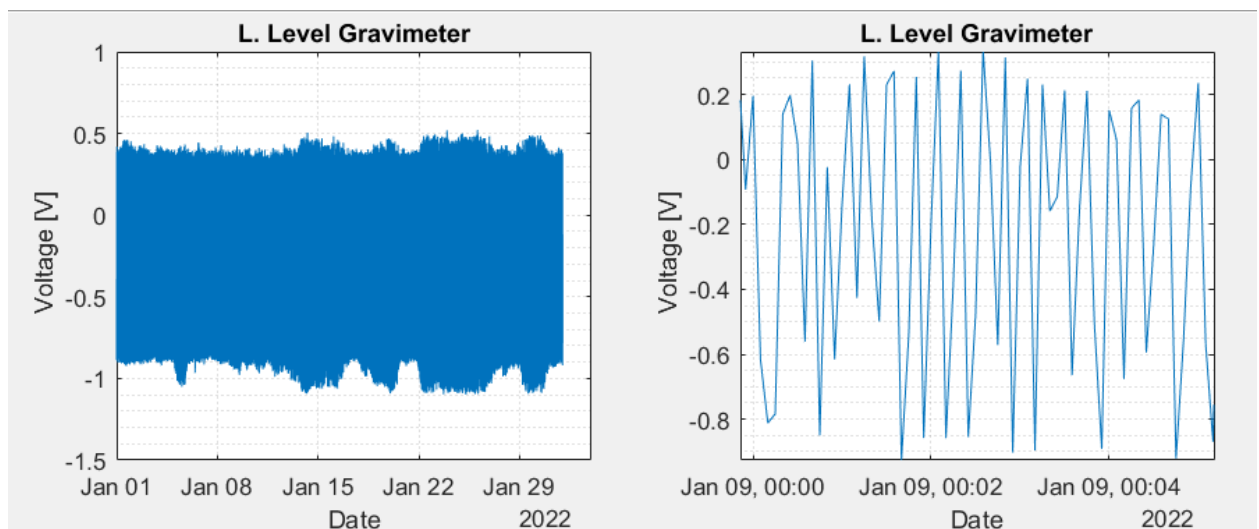


Figure 54. Lateral Level Signal Monitoring

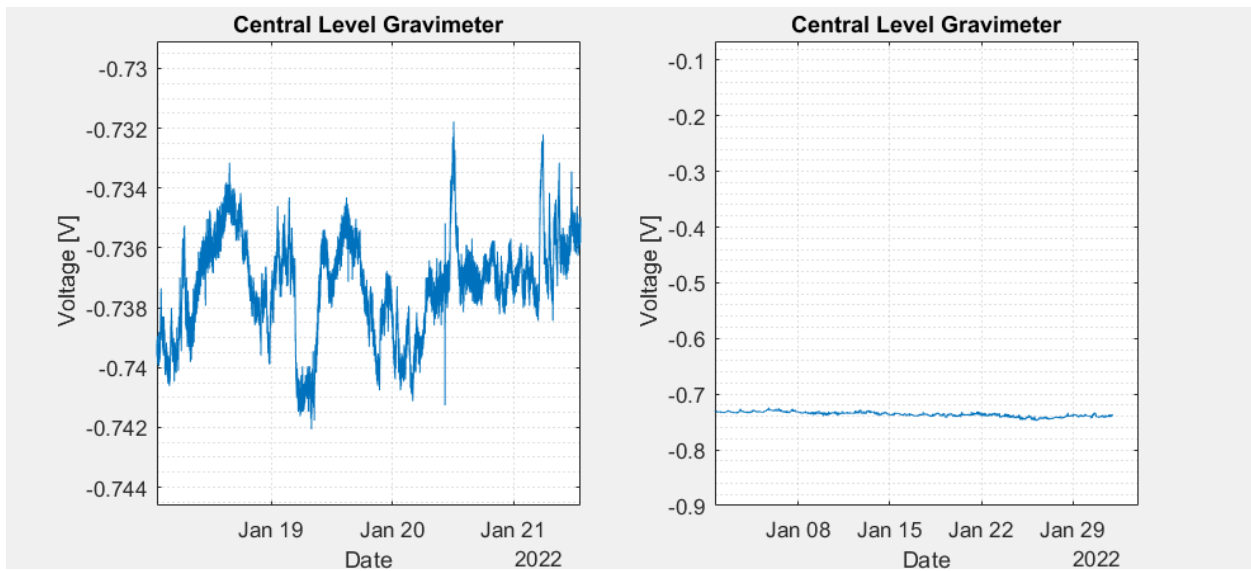


Figure 55. Central Level Signal Monitoring

The system also monitored the power supply during the whole testing period. As it can be shown on figures 56 and 57 and the voltage maintained constant around the +12.0 V / -12.0 V ad required within a 1% accuracy.

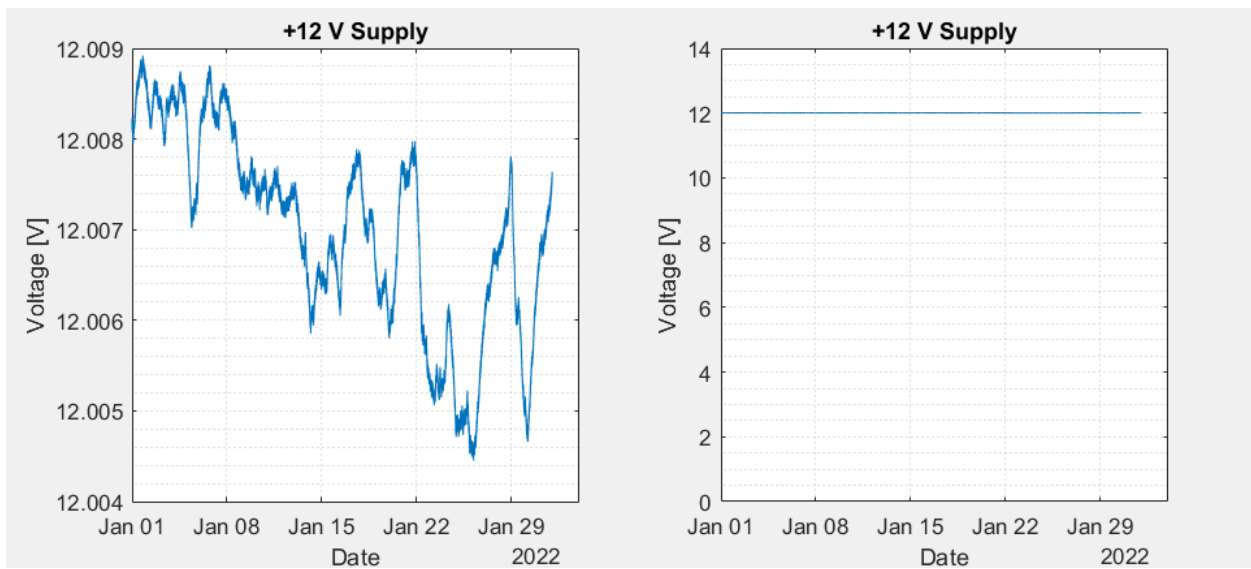


Figure 56.. +12 V Supply Monitoring

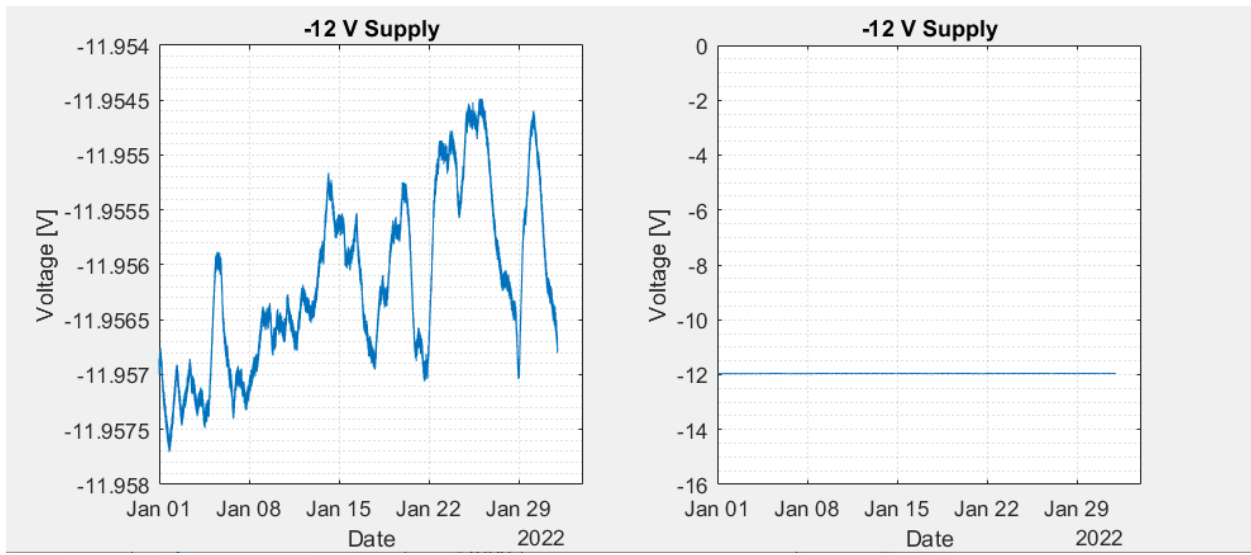


Figure 57. -12 V Supply Monitoring

As it can be seen on these examples, the Agilent Switching unit provided monitoring with a variable range of between -20V to 20 V with resolution of 6.5 decimal places or $0.5\mu\text{V}$. And an accuracy of with 0.004%. Commercial acquisition cards like the NI myRIO-1900 from National Instruments have a resolution up to 12 bits (National Instruments).

4. Confrontation with tidal monitoring from a different station:

As it can be observed on Figure 58, when compared to the actual tidal fluctuations on earth's oceans, The measured results (upper right) closely follow the theoretical approximation (lower right) and at the left, the Fourier transform with the frequency peaks is as expected for tidal monitoring:

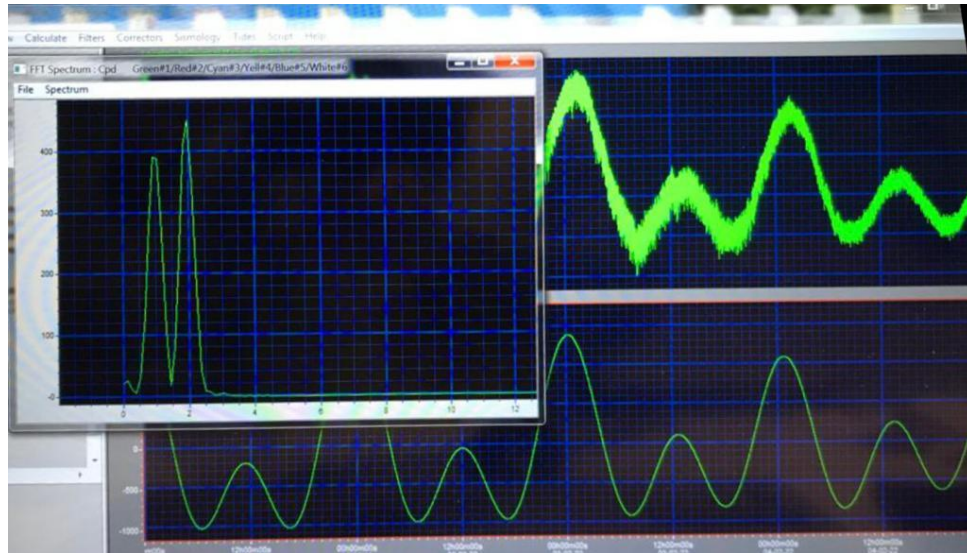


Figure 58. Gravimetric Variation based on theoretical tidal fluctuation.

CHAPTER 4: CONCLUSIONS

As demonstrated on the results section, the expected accuracy of the gravitational monitoring system proved to be exceptional. The Agilent switching unit with 22 bits of resolution (while common data acquisition devices have 8-to-12-bit resolution) and a 6.5 decimal digit precision with 0.04% accuracy proved to be a perfect match for the LaCoste & Romberg Model G-1089 gravimetry, as this brand has been highly placed amongst research on the field due to its high-quality gravimeter and development of sensors in the last in the last 40 years. The brand has been known for its high quality at a steep price.

Further considerations were also done as the delay that the Agilent Switching unit introduced a delay in the order of the 200 milliseconds. However, it was not deemed significant, as the sampling period is 5 seconds while and in the worst-case scenarios the delay represents only a 2% of this sampling period. Furthermore, the gravity fluctuation due to the tidal change in planet earth follows a variation with a frequency of around 1 day, furthermore, negating the importance of a 200-millisecond delay with so slow changing parameters.

Future improvements could be introducing new barometers and thermometers to the gravitational station. Although the information that is used not being directly measured is close enough to the new metrological station, further implementation, and variety of should be aimed for. Thankfully, the system allows several possibilities for expansion. Internet connection for live monitoring is also in the apriority to easy access to the data generated and useful in integration to larger metrological networks.

BIBLIOGRAPHY

- A. Albano, G. C. (2015, March). Continuous gravity and tilt observations in an active geodynamic area of southern Italy: the Calabrian Arc system. *56*, 1-18.
- A. Cazenave, K. S. (2009). Sea level budget over 2003–2008: A reevaluation from GRACE space gravimetry, satellite altimetry and Argo. *Global and Planetary Change*, *65*(2-1).
- A. Thomas J. Gebhart. (1994). Correlations between gravimetry and light scattering photometry for atmospheric aerosols. *Atmospheric Environment*, *28*(5).
- Agilent . (n.d.). *Agilent Technologies. Agilent 34970A Data Acquisition and Switching Unit manual*. Retrieved from <https://www.avionteq.com/document/34901A-specification-sheet.pdf>
- Aline Peltiera, P. B. (2011). Early detection of large eruptions at Piton de La Fournaise volcano (La Réunion Island): Contribution of a distant tiltmeter station. *Journal of Volcanology and Geothermal Research*, *199*(1-2), 96-104.
- Applied Geomechanics. (n.d.). *700-Series Platform and Sufca Mount Tiltmeters. User Manual* .
- B Richter, H. W. (2013). The Frankfurt calibration system for relative gravimeters. *IOP Publishing Ltd*, *3*(32), 217.
- Biolcati E., O. O. (2013). Absolute measurements of the free-fall . *Metrologica, INRiM, Torino, Italy, Technical Report* , *29*, 13.
- Carlos Duque, M. L.-R.-C. (2008). Combined time domain electromagnetic soundings and gravimetry to determine marine intrusion in a detrital coastal aquifer (Southern Spain). *Journal of Hydrology*, *349*(3-4), Pages 536-547,.
- D. Zhong, R. K. (2013). Comparison of Methods for Determination of the Vertical Acceleration in Airborne Gravimetry Using LaCoste & Romberg Zero Length Spring Gravimeter. *Proceedings of the 26th International Technical Meeting of the Satellite Division of The Institute of Navigation*, 3180 - 3193.
- G. D'Agostino, A. G. (2005). A method to estimate the time–position coordinates of a free-falling test-mass in absolute gravimetry. *BIPM and IOP Publishing Ltd*, *42*(4), 233.

- G.G.O. Lopes Cardozo, J. E. (2005). Detection of active crustal structures in the Upper Rhine Graben using local earthquake tomography, gravimetry and reflection,. *Sismic Quaternary Science Reviews*, 24,(Issues 3–4,), Pages 337-344,.
- J. C. Harrison, T. S. (1984). Implementation of electrostatic feedback with a LaCoste-Romberg Model G Gravity Meter. *Journal of Geophysical Reaserch Solid Earth*, 89(B9), 7957-7961.
- Jie Liu, W.-J. X.-K.-K. (2022). Sensitive quantum tiltmeter with nanoradian resolution. *Physics Review*.
- Jing Tong, X. Z. (2018). Marine strata morphology of the South Yellow Sea based on high-resolution aeromagnetic and airborne gravity data. *Marine and Petroleum Geology*, 96, 429-440.
- Keysight. (n.d.). *Service Manuals. 34970A/34972A Data Acquisition / Switch Unit Service Guide*. Retrieved from <https://www.keysight.com/it/en/assets/9018-02645/service-manuals/9018-02645.pdf>
- L. Kallivroussis, A. N. (2002). RD—Rural Development: The Energy Balance of Sunflower Production for Biodiesel in Greece,. *Biosystems Engineering*, 24(3-4), 347-354,.
- LacCste And Romberg. (2004). *A New Generation Dynamic Gravity Meter Manual*. Retrieved 2022, from <http://www.lacosteromberg.com/pdf/airSea.pdf>
- LaCoste, L. J. (1935). A simplification in the conditions for the zero-length-spring seismograph. *Bulletin of the Seismological Society of America*, 25(2), 176–179.
- LaCoste, L. (n.d.). The zero-length spring gravity meter. *The Leading Edge*, 7(7).
- LaCoste, M. G. (2006). *FG5 Automatic Gravimetes Users Manual*. Retrieved 2022, from <http://www.lacosteromberg.com/pdf/FG5Manual2007.pdf>
- McCulloh, T. H. (1966). The promise of precise borehole gravimetry in petroleum exploration and exploitation. *U.S. Geological Survey*.
- Moradi, P., Angus, D., & Sharma, M. (2022). Hydraulic Fracture Width Inversion Using Simultaneous Downhole Tiltmeter and Distributed Acoustic Sensing Data.

- National Instruments. (n.d.). *USER GUIDE AND SPECIFICATIONS NI myRIO-1900*. Retrieved from <https://www.ni.com/pdf/manuals/376047c.pdf>
- Olesen, A. V. (2022). . "Improved airborne scalar gravimetry for regional gravity field mapping and geoid determination. *Copenhagen: University of Copenhagen*.
- Pater, C. J., Koning, J. d., Maxwell, S. C., & Walters, D. A. (2008.). Geomechanics for interpreting SAGD monitoring using micro-seismicity and surface tiltmeters. *aper presented at the International Thermal Operations and Heavy Oil Symposium, Calgary, Alberta, Canada,.*
- Peters, W. C. (1987). *Exploration and mining geology*. Second edition. 2.
- R. Sulzbach, H. D. (2021). High-Resolution Numerical Modeling of Barotropic Global Ocean Tides for Satellite Gravimetry. *5(126)*.
- Review of Scientific Instruments. (2008). A silica long base tiltmeter with high stability and resolution. *79(3)*.
- Simpson, J. E. (1982). Gravity Currents in the Laboratory, Atmosphere, and Ocean. *Annual Review of Fluid Mechanics, 14*, 213-2016.
- Snadden, M. J. (1998). Measurement of the Earth's gravity gradient with an atom interferometer-based gravity gradiometer. *Physical review letters, 81.5*, 971.
- T.M.Niebauer, J. M. (2011). Monitoring earthquakes with gravity meters. *Geodesy and Geodynamics, 2(3)*, 71-75.
- Timmen, L. (2010). Absolute and relative gravimetry . *Sciences of Geodesy*, 1-48.
- V.Cayol, F. H. (1997). 3D mixed boundary elements for elastostatic deformation field analysis. *International Journal of Rock Mechanics and Mining Sciences, 34(2)*, 275-287.
- Vajda, P. (2016). Recent Developments and Trends in Volcano Gravimetry. *Chapter Metric Overview*.
- Woollard, G. (1959). Crustal structure from gravity and seismic measurements. *64(10)*, 1521-1544.

World Documents. LaCoste & Romberg Gravimeters. (2015). Retrieved 2022, from <https://vdocuments.net/lacoste-romberg-gravimetro.html>